Dark Matter Axion Group

cea iramis spec Fermilab

INFN PADOVA
Istituto Nazionale di Fisica Nucleare
Sezione di Padova

INFN LNL
Istituto Nazionale di Fisica Nucleare
Laboratori Nazionali di Legnaro

Status and Prospects of QUaere AXion at Laboratori Nazionali di Legnaro

Danho Ahn (on behalf of QUAX-PD/LNL)

Sezione di Padova, Instituto Nazionale di Fisca Nucleare, Padova 35131, Italy

Contents

Status and Prospects of QUAX-PD/LNL

Introduction

Strong CP Problem and Composition of Dark Matter

1. The strong CP problem

$$\mathcal{L}_\theta = \bar{\theta}\ \frac{g_s^2}{32\pi^2}\ G^a_{\mu\nu}\ \tilde{G}^{a\mu\nu}$$

Weinberg (1975); 't Hooft (1976)

- This term violates CP in QCD.
- It induces a neutron electric dipole moment.
- Experiments imply $|\bar{\theta}| \lesssim 10^{-10}$.

$$d_n \approx (1-3) \times 10^{-16}\ \bar{\theta}\ e \cdot cm$$

representative hadronic estimate

Crewther *et al.* (1979); Pospelov & Ritz (2005)

Why does a permanent neutron EDM violate P and T?

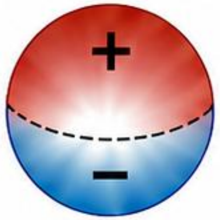

neutron

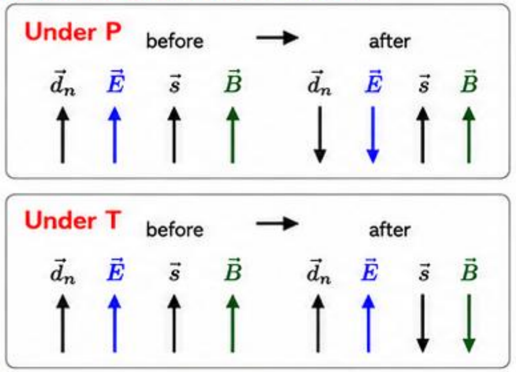

$$\Delta E = -\vec{d}_n \cdot \vec{E} - \vec{\mu}_n \cdot \vec{B}$$

Baker *et al.* (2006); Abel *et al.* (2020)

Why is $\bar{\theta}$ so small? This is the strong CP problem.

2. What is dark matter made of?

Dark matter certainly exists observationally,
but its microscopic particle nature is still unknown.

Galaxy rotation curves

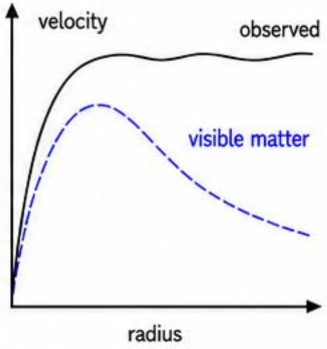

Rubin, Thonnard & Ford (1980)

Gravitational lensing

Clowe *et al.* (2006)

CMB / large-scale structure

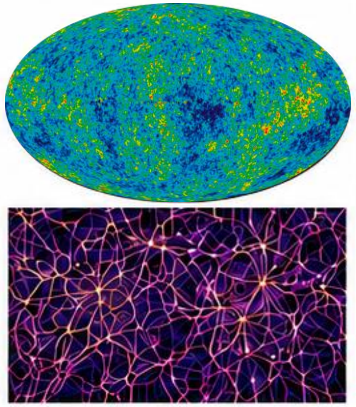

Planck Collaboration (2020)

**We know dark matter is there,
but we still do not know which particle it is made of.**

Introduction

Axion can solve strong CP problem

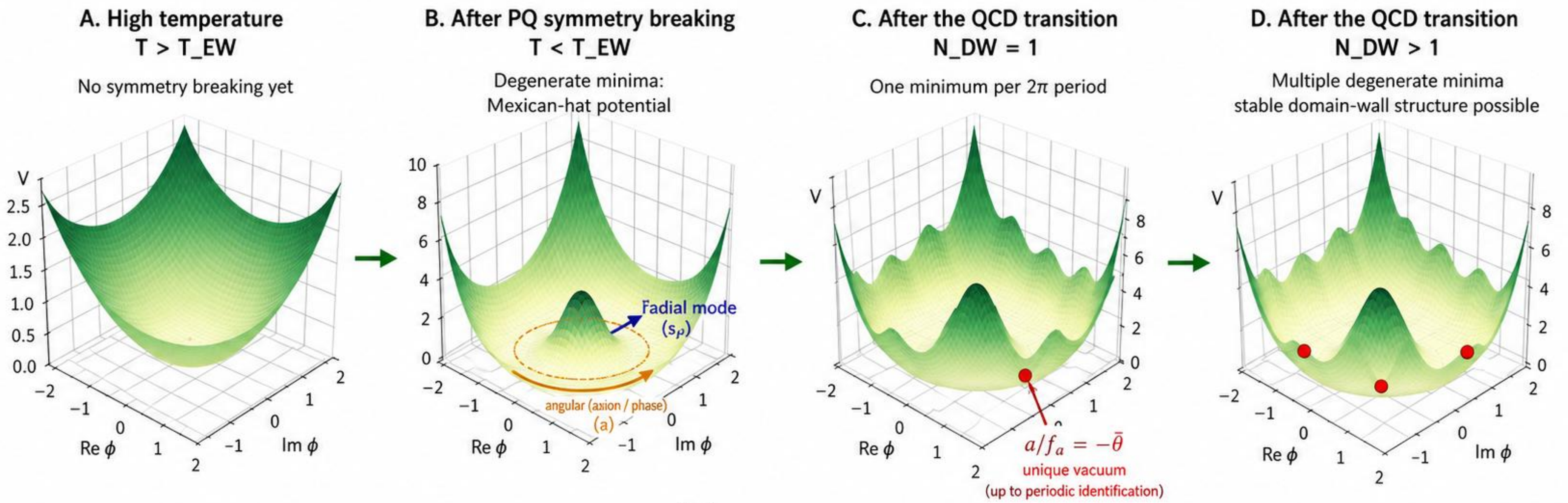

$$V(\phi, T) = m^2(T)|\phi|^2 + \lambda|\phi|^4$$
$$m^2(T) > 0$$

$$V(\phi, T) = \lambda\left(|\phi|^2 - \frac{v(T)^2}{2}\right)^2$$

$$V(a) \simeq \chi(T)\left[1 - \cos\left(\frac{a}{f_a} + \bar{\theta}\right)\right]$$

$$V(a) \simeq \chi(T)\left[1 - \cos\left(\frac{N_{\rm DW}a}{f_a} + \bar{\theta}\right)\right]$$

QCD generates the axion potential. For $N_{DW} = 1$ the vacuum is unique and the axion relaxes the effective $\bar{\theta}$ angle, solving the strong CP problem. For $N_{DW} > 1$ several degenerate vacua appear.

Refs. R.D. Peccei & H.R. Quinn, Phys. Rev. Lett. 38, 1440 (1977); S. Weinberg, Phys. Rev. Lett. 40, 223 (1978); F. Wilczek, Phys. Rev. Lett. 40, 279 (1978); L. Di Luzio *et al.*, Phys. Rept. 870, 1 (2020).

Introduction

Axion is a dark matter candidate

https://cajohare.github.io/AxionLimits/

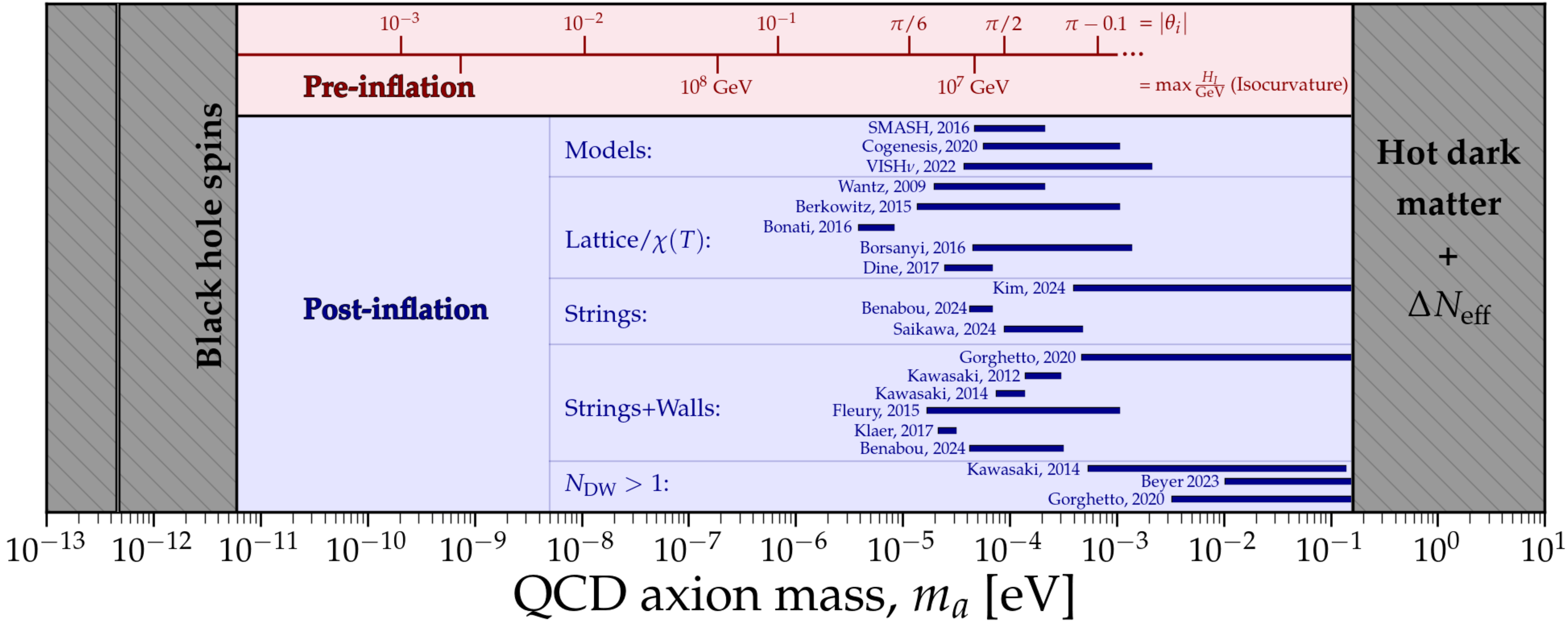

Introduction

Axion is a dark matter candidate

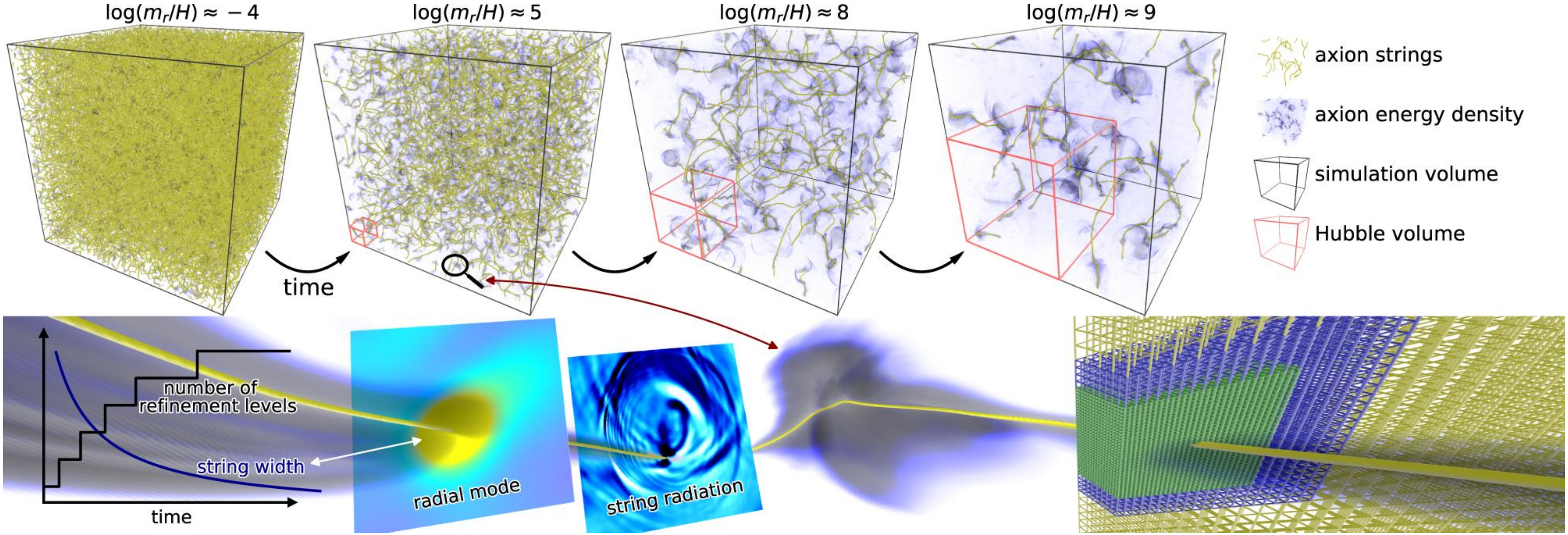

Buschmann *et al*. (2022)

Introduction

Axion is a dark matter candidate

https://cajohare.github.io/AxionLimits/

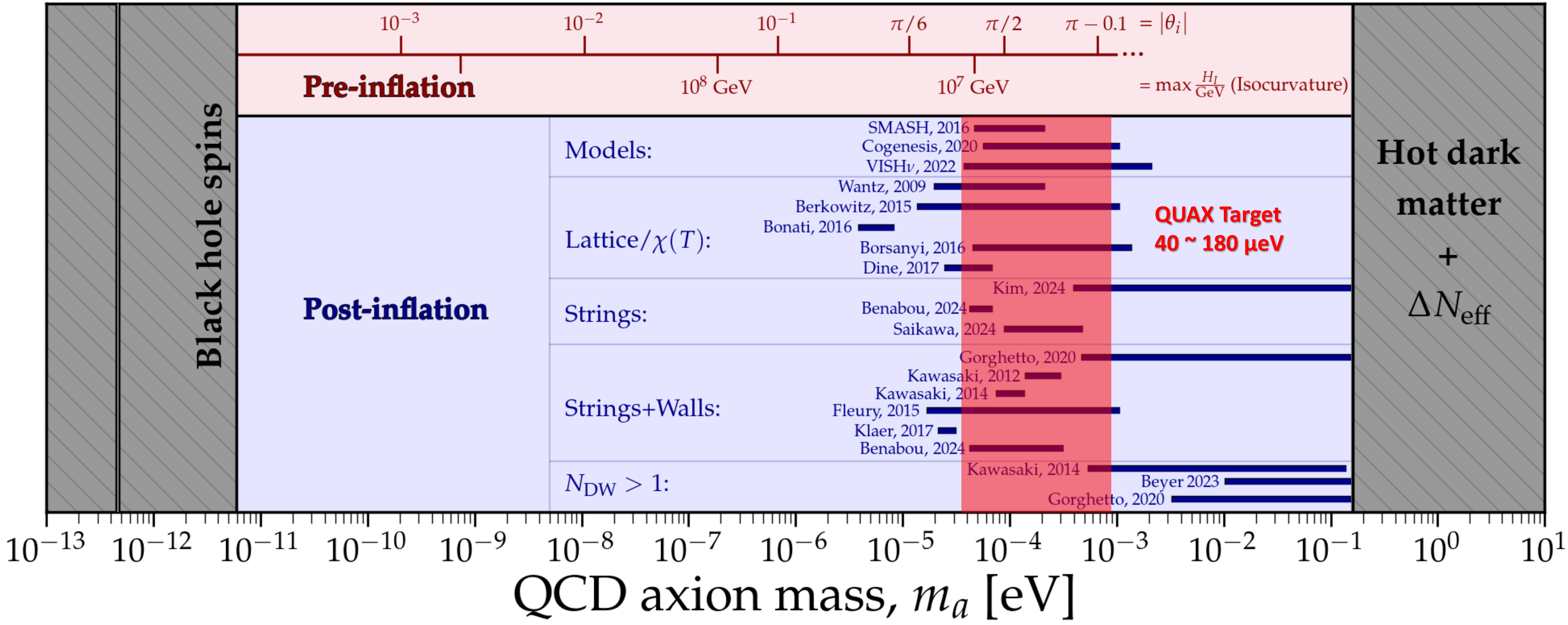

Introduction

Axion in the low energy regime

A. Axion – Photon Coupling ($a \to \gamma\gamma$)

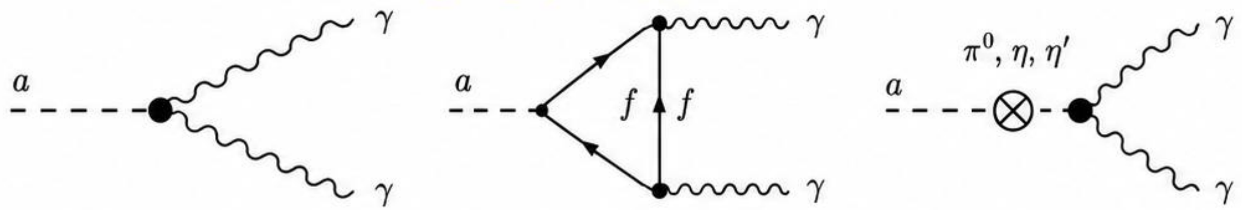

effective vertex — charged-fermion triangle — meson mixing (QCD axion)

Model	E/N	g_γ ($C_{\rm QCD} = 1.92(4)$)	g_γ ($C_{\rm QCD} \approx 1.77(8)$)
KSVZ (minimal)	0	-0.96	-0.885
DFSZ (canonical)	8/3	$+0.373$	$+0.448$

$$g_{a\gamma\gamma} = \frac{\alpha}{2\pi f_a}\left(\frac{E}{N} - C_{\rm QCD}\right) = \frac{\alpha}{\pi f_a}\, g_\gamma$$

lattice QCD update: $C_{\rm QCD} \approx 1.77(8)$ (vs standard $1.92(4)$)

B. Axion – Electron Coupling ($a \to e^+e^-$)

derivative coupling

$$\frac{C_e}{2 f_a}\,(\partial_\mu a)\,\bar{e}\gamma^\mu\gamma^5 e$$

pseudoscalar form

$$-i g_{ae}\, a\, \bar{e}\gamma^5 e$$

$$g_{ae} = C_e \frac{m_e}{f_a}$$

KSVZ

$C_e = 0$ (tree level)

RG-induced: $C_e \sim 0.8 \times 10^{-3}$

$g_{ae} \sim 4.1 \times 10^{-19}$ ($f_a = 10^{12}$ GeV)

DFSZ

DFSZ-I: $C_e = +\frac{1}{3}\sin^2\beta$

DFSZ-II: $C_e = -\frac{1}{3}\cos^2\beta$

β

$\tan\beta = v_u/v_d$

$\tan\beta = 1 \Rightarrow \sin^2\beta = \cos^2\beta = \frac{1}{2}$

$C_e = \pm\frac{1}{6}$

$g_{ae} = \pm 8.52 \times 10^{-17}$ ($f_a = 10^{12}$ GeV)

Refs: di Cortona et al. (2016); Bauer et al. (2021); Choi et al. (2021); Jaeckel & Thormaehlen (2019).

Introduction

Ferromagnetic Haloscope - QUAX-g_{ae}

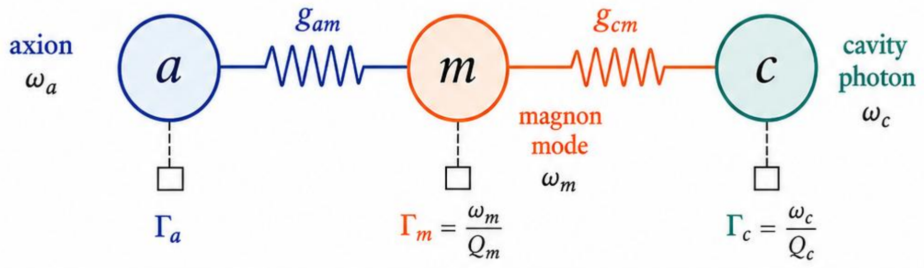

Coupled oscillator / multimode Hamiltonian

$$\hat{H} = \sum_i \hbar\left(\omega_{c,i} - i\frac{\gamma_{c,i}}{2}\right) a_i^\dagger a_i + \sum_j \hbar\left(\omega_{m,j} - i\frac{\gamma_{m,j}}{2}\right) m_j^\dagger m_j + \sum_{i,j} \hbar g_{ij}\left(a_i^\dagger m_j + a_i m_j^\dagger\right)$$

Example values used in the B_a and P_a estimates

m_a	=	$42\ \mu\text{eV}$
g_{aee}	=	1.0×10^{-15} *(benchmark, model dependent)*
v_a	=	220 km/s $\approx 7.3 \times 10^{-4}\,c$
ρ_a	=	0.45 GeV/cm^3
n_a	=	$\rho_a/(m_a c^2) \approx 1.1 \times 10^{13}$ cm^{-3}
n_s	=	1.0×10^{22} cm^{-3} (YIG spin density)
V_m	=	4.8×10^{-2} cm^3 ([illegible]pheres, diameter 2.1 mm)
N_s	=	$n_s V_m \approx 4.8 \times 10^{20}$
ω_a	=	6.4×10^{10} s^{-1} ($\approx 2\pi \times 10.2$ GHz)
τ_s	=	1.0×10^{-6} s
B_a	$\approx$	4×10^{-23} T

Values are benchmark inputs for order-of-magnitude estimates.

Axion signal power

$$\mathcal{L}_{ae} \simeq -2\mu_B\,\boldsymbol{\sigma}\cdot\left(\frac{g_{aee}}{2e}\nabla a\right) \equiv -2\mu_B\,\boldsymbol{\sigma}\cdot\boldsymbol{B}_a$$

$$B_a = \frac{g_{aee}}{2e}\sqrt{\frac{n_a\hbar}{m_a c}}\, m_a v_a \simeq 4\times10^{-23}\left(\frac{m_a}{42\ \mu\text{eV}}\right)\text{T}$$

$$P_a = \gamma_e \mu_B N_s\, \omega_a\, B_a^2\, \tau_s$$

Example estimate: $P_a \approx 1 \times 10^{-31}$ W

References: Crescini et al., *Phys. Dark Universe* **15**, 135–141 (2017); *Phys. Rev. Lett.* **124**, 171801 (2020); *Commun. Phys.* **3**, 164 (2020); *Phys. Rev. B* **104**, 064426 (2021).

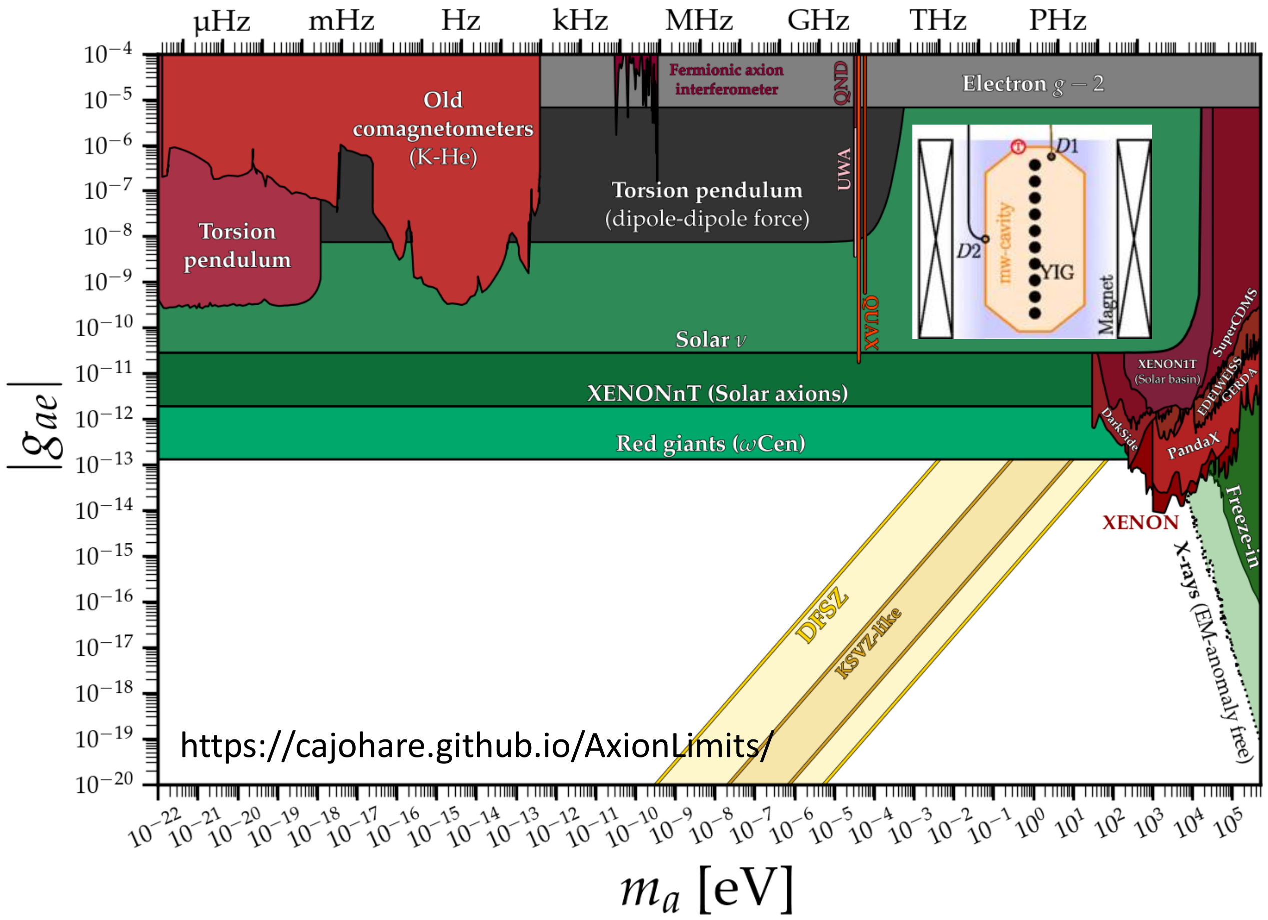

Introduction

Ferromagnetic Haloscope - QUAX-g_{ae}

C. Braggio, Presented at the STDM Conference, Rome, Italy

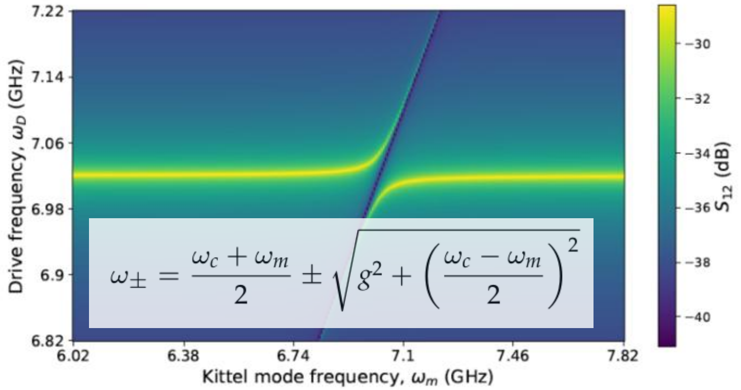

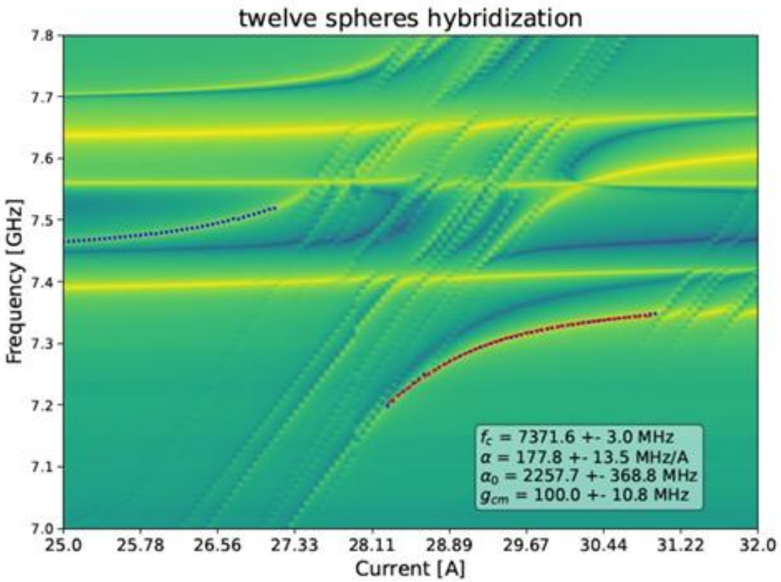

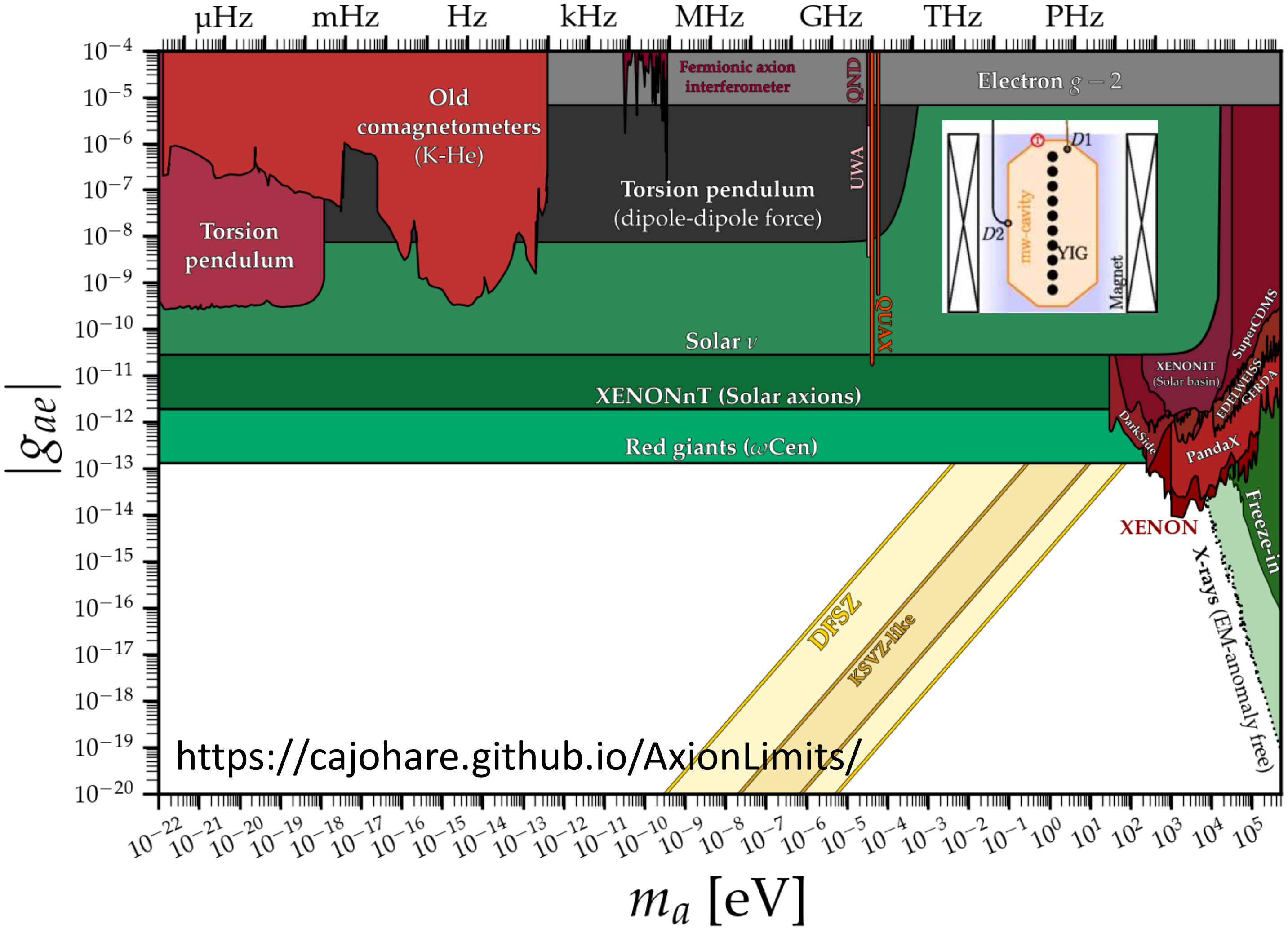

Introduction

Axion Haloscope - QUAX-$g_{a\gamma}$

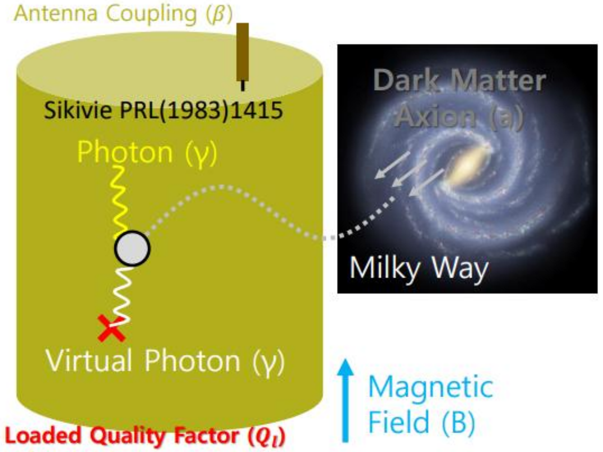

Loaded Quality Factor (Q_l)
Volume (V)
Resonant Angular Frequency ($\omega_0 \sim m_a$)
Form Factor ($C \sim \int E_m \cdot B\, dV$)
System Temperature (T_{sys})

Signal Power; Coupling Constant; Dark Matter Axion Density

$$P_{sig} = \frac{\beta}{1+\beta} g_{a\gamma\gamma}^2 \frac{\rho_a}{m_a^2} \mathbf{B^2} V \omega_0 C \frac{Q_a \mathbf{Q_l}}{Q_a + \mathbf{Q_l}}$$

Axion Mass; Axion Quality Factor

Kim *et al*. JCAP03(2020)066

Scanning speed

$$\frac{df}{dt} \propto \frac{\mathbf{B^4} V^2 C^2}{k_B^2 T_{sys}^2} \mathbf{Q_l} Q_a$$

$\mathbf{Q_l} \gg Q_a \sim 10^6$

System Noise Temperature

Kim, Patras Workshop, 2023

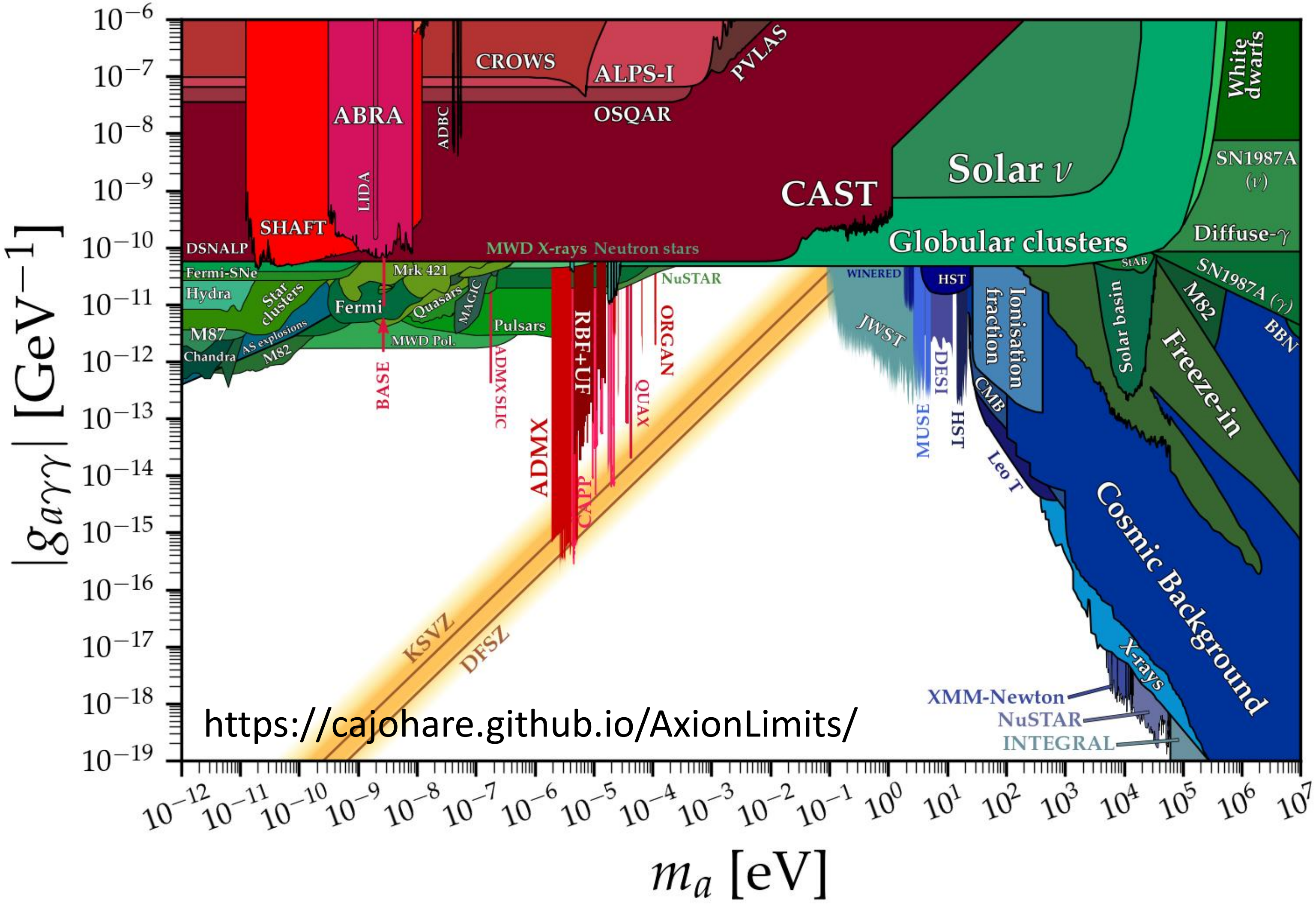

Introduction

QUaerere AXion (QUAX)

G. Ruoso, Presented at the STDM Conference, Rome, Italy

- In 2020 **INFN** has financed the **QUAX** experiment to run an observatory for searching axion via the **axion-photon coupling in the unexplored region around 10 GHz**

- **QUAX** is based on **two haloscopes**: one in Legnaro/Padova (LNL) and the other in Frascati (LNF)

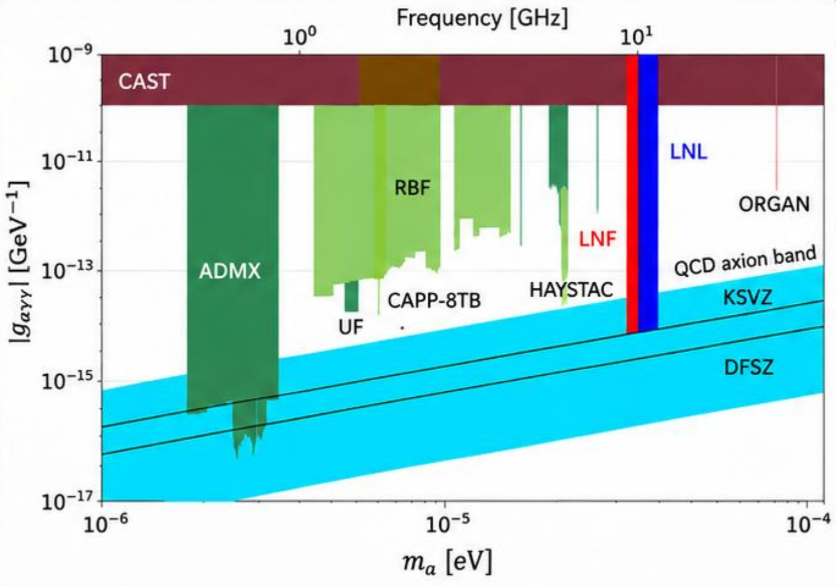

	LNF (Frascati)	LNL (Legnaro/Padova)
Magnetic field	9 T	14 T
Magnet length	40 cm	50 cm
Magnet inner diameter	9 cm	12 cm
Frequency range	8.5 – 10 GHz	9.5 – 11 GHz
Cavity type	Hybrid SC	Dielectric
Scanning type	Inserted rod	Mobile cylinder
Number of cavities	7	1
Cavity length	0.3 m	0.4 m
Cavity diameter	25.5 mm	58 mm
Cavity mode	TM010	pseudo-TM030
Single volume	$1.5 \cdot 10^{-4}$ m^3	$1.5 \cdot 10^{-4}$ m^3
Total volume	7 × 0.15 liters	0.15 liters
Q_0	300 000	1 000 000
Single scan bandwidth	630 kHz	30 kHz
Axion power	$7 \times 1.2 \cdot 10^{-23}$ W	$0.99 \cdot 10^{-22}$ W
Preamplifier	TWJPA/INRIM	DJJAA/Grenoble
Operating temperature	30 mK	30 mK

- The **LNL/PD haloscope** will be based on dielectric loaded cavities, traveling wave parametric amplifiers and **14 T magnet**

Introduction

QUAX-PD/LNL Infrastructure

QUAX-BLU	QUAX-LNL	QUAX-RED
10 mK	Sub-100 mK	Sub-100 mK
9 T Magnet	9 T Magnet	14 T Magnet
Single Microwave Photon Counter	Quantum-Limited Noise Amplifier	Quantum-Limited Noise Amplifier
Axion/Ferromagnetic Haloscope	Axion Haloscope	Axion Haloscope, Dark Photon

QUAX-LNL Haloscope

Dilution Refrigerator

QUAX main criostat with gas handling system and safety control

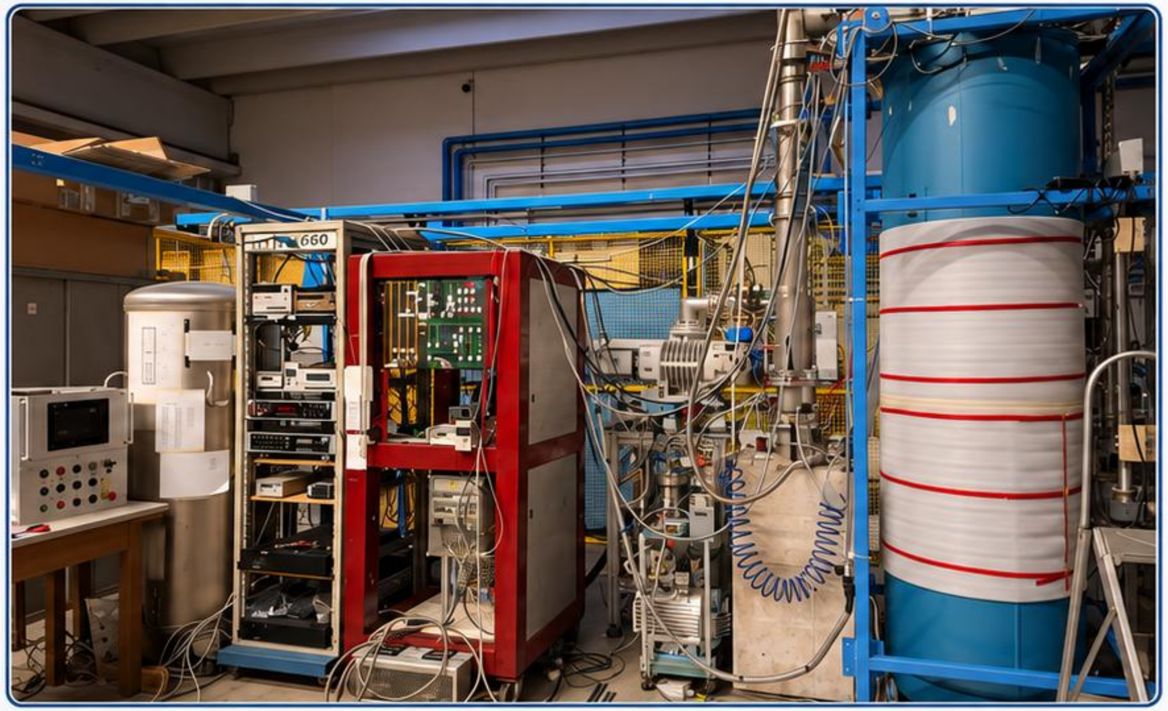

- Main dewar: 2800 mm height, 500 mm inner diameter
- Two weeks operation: ~3000 liters of liquid helium
- Refurbished **wet dilution unit** from AURIGA experiment
- Base temperature @ MC 60 mK
- Cavity and electronics kept @ 120 mK

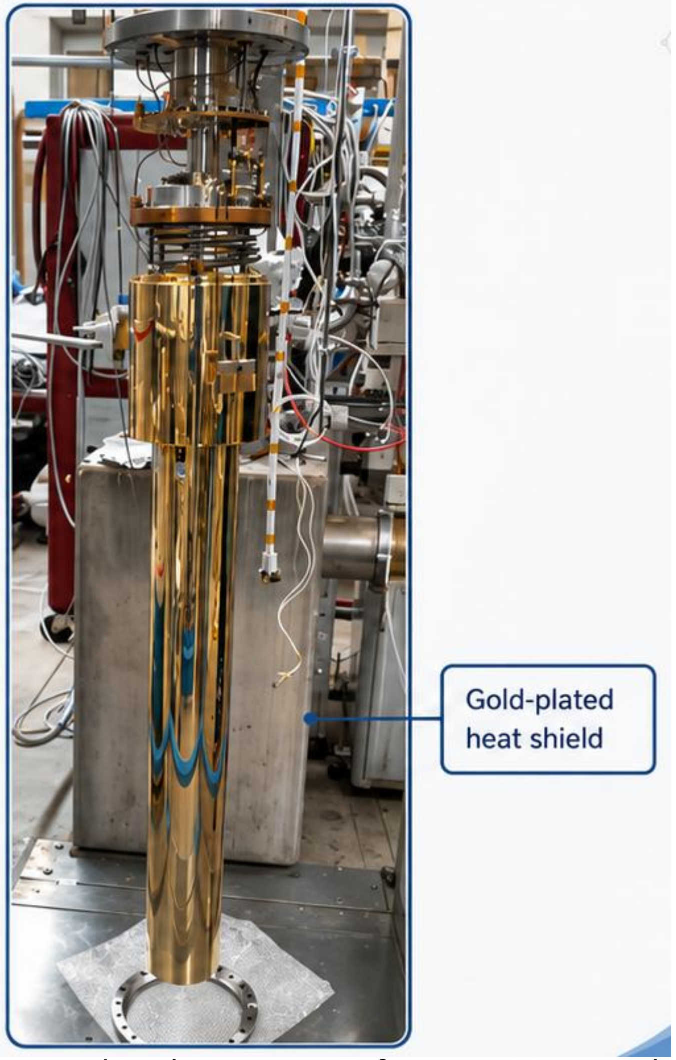

G. Ruoso, Presented at the STDM Conference, Rome, Italy

QUAX-LNL Haloscope

Dielectrically Loaded Tunable Cavity

Cavity parts

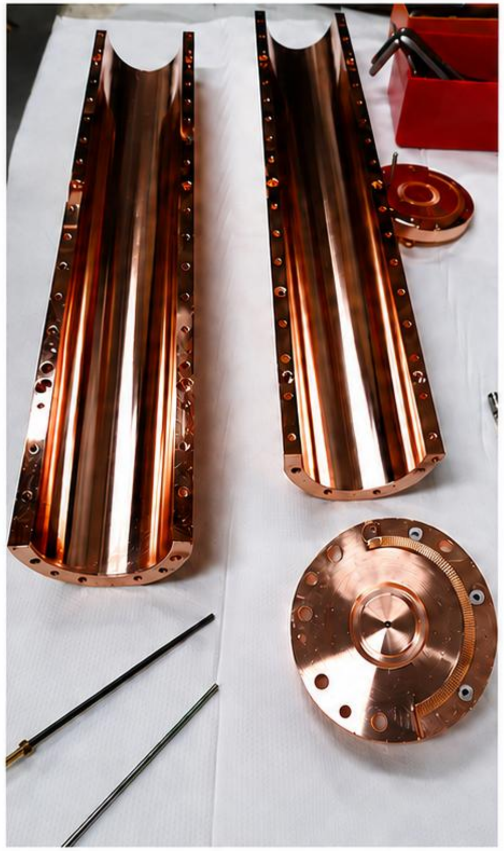

Endcap with RF sliding contacts
and sapphire holding grooves

Clamshell mechanism for tuning

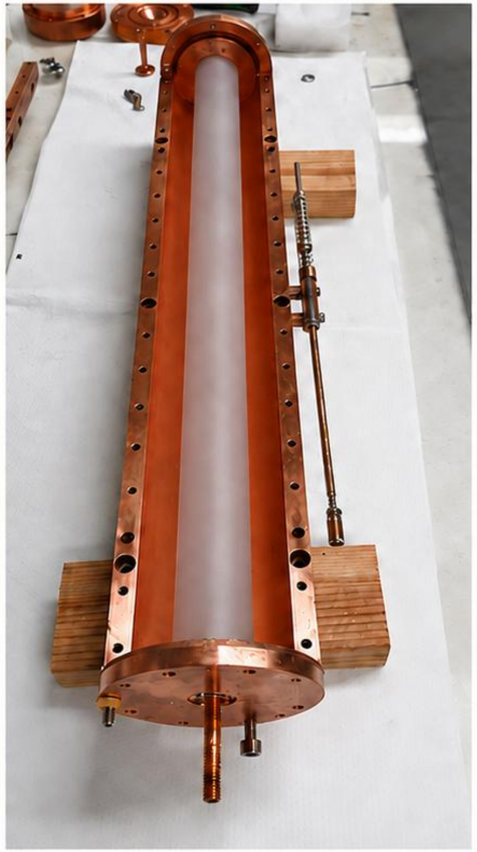

Open cavity with sapphire cylinder

Concept and specifications

- Right cylindrical hybrid cavity
- TM030 mode for large volume
- Copper shell
- Hollow sapphire cylinder inside

- **LAMED TC:** tunable cavity
  "LAMED" from the Phoenician
  letter meaning "goad"

- **Base frequency:** 10.2 GHz
- **Inner length:** 413.4 mm
- **Inner diameter:** 60.5 mm
- **Volume:** 1.17 liters

RF antenna

G. Ruoso, Presented at the STDM Conference, Rome, Italy

QUAX-LNL Haloscope

Dielectrically Loaded Tunable Cavity

LAMED-TC

name derived from the Phoenician letter meaning 'goad'

End cap details

Pantograph

- Inner length = **413.4 mm**
- Inner diameter = **60.5 mm**
- Volume = **1.17 liters**
- C_{030} = **0.43**

- Frame OFHC copper
- L = 420 mm sapphire cylinder (from Armenia)
- Movable side wall – clamshell mechanism
- Single-body endcaps
- Endcaps with 5.3 mm deep grooves for sapphire holding
- Copper RF sliding contacts
- Motor-actuated pantograph-like aperture mechanism
- Teflon 1.1 mm diameter to keep sapphire centered
- **Science mode TM030**
- Tuning 85 MHz
- Q0 ~ 80,000

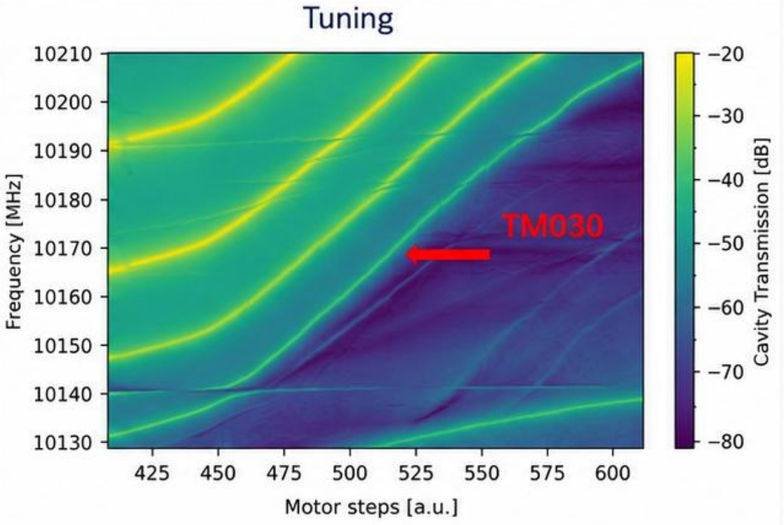

G. Ruoso, Presented at the STDM Conference, Rome, Italy

QUAX-LNL Haloscope

Magnet

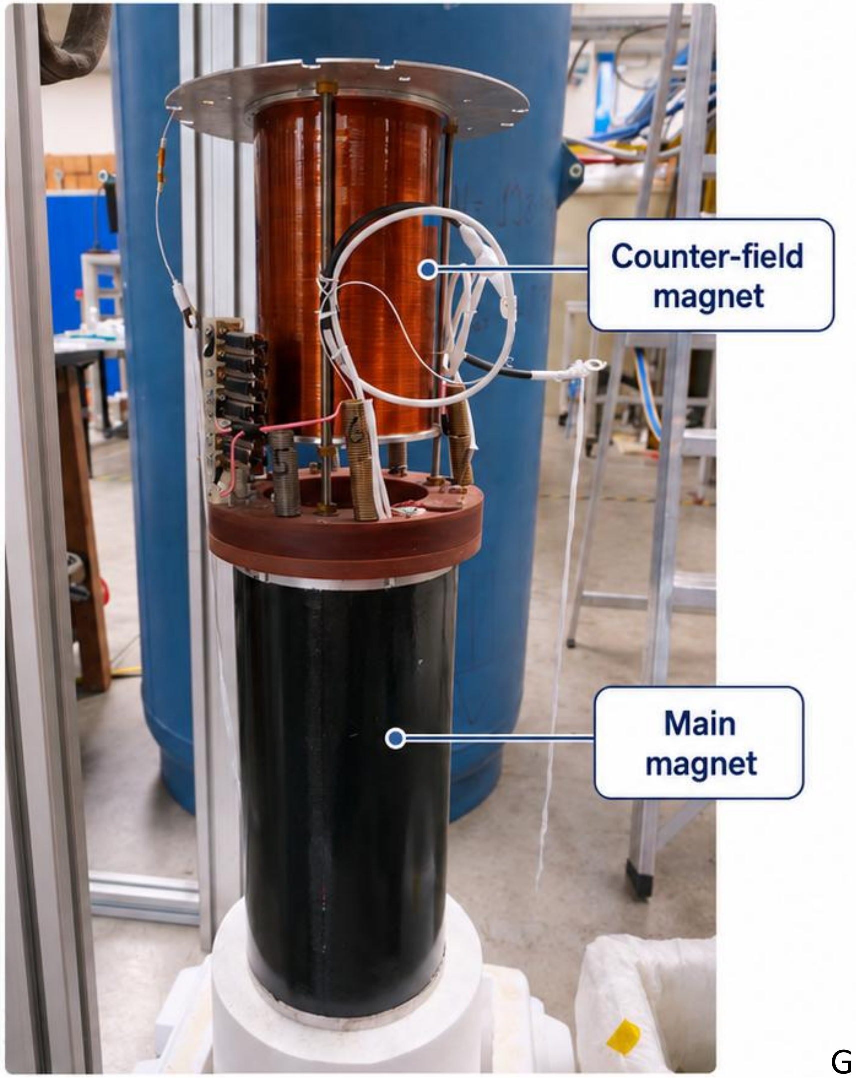

Counter-field magnet

- NbTi superconducting coil
- Inner diameter **150 mm,** height **250 mm**
- Same driving current as the main magnet
- Reduces stray field below **40 mT** on sensitive electronics (also passively shielded)

Main magnet

- NbTi superconducting coil
- Length **450 mm**, inner diameter **150 mm**
- Peak field **8.0 T @ 92 A** current
- Square field integral **50.2 T^2 m**

G. Ruoso, Presented at the STDM Conference, Rome, Italy

QUAX-LNL Haloscope

RF Receiver

High frequency receiver working in a strong magnetic field environment

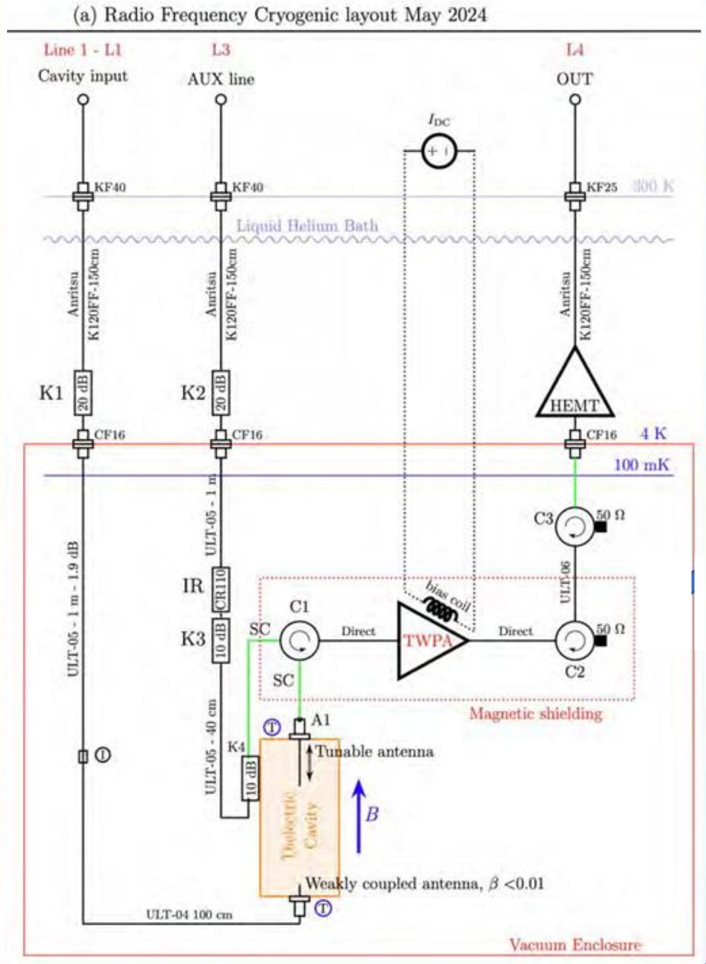

The 10 GHz low noise receiver is based on a Travelling Wave Parametric Amplifier (TWPA - from N. Roch, Grenoble)

A. Ranadive, et al., *Nat. Commun. 13, 1737 (2022)*

RF chain in magnetic shielding box

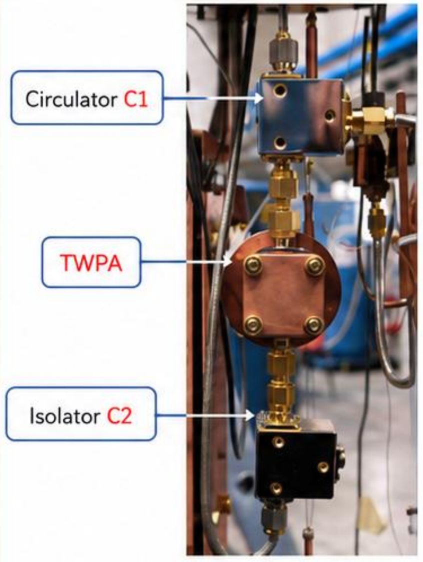

Inside

Detail of DU insert

TWPA is made by superconducting Aluminum Josephson Junction arrays, very sensitive to ambient magnetic field

Two-layers passive shielding: CRYOPERM (inside) + lead

G. Ruoso, Presented at the STDM Conference, Rome, Italy

QUAX-LNL Haloscope

Travelling Wave Parametric Amplifier (TWPA) Operation

- **four wewe mixing TWPA** with a phase matching process based on the sign reversal of the third order (Kerr) nonlinearity of a series of Josephson Junctions arrays (A. Ranadive, et al., *Nat. Commun. 13, 1737 (2022)*)
- TWPA amplification controlled by **intensity I_p** and **frequency f_p** of the pump tone and **current I_b** of a biasing magnetic field

(a) TWPA ON/OFF Gain

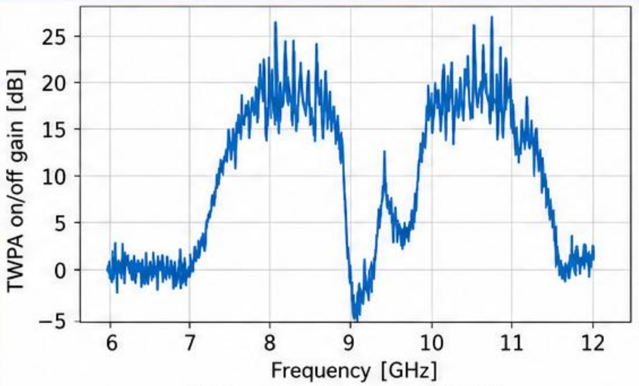

Gain curve for f_p = 9.35 GHz

Single ripple

In order to maximize SNR one has to tune the gain profile of the TWPA amplifier

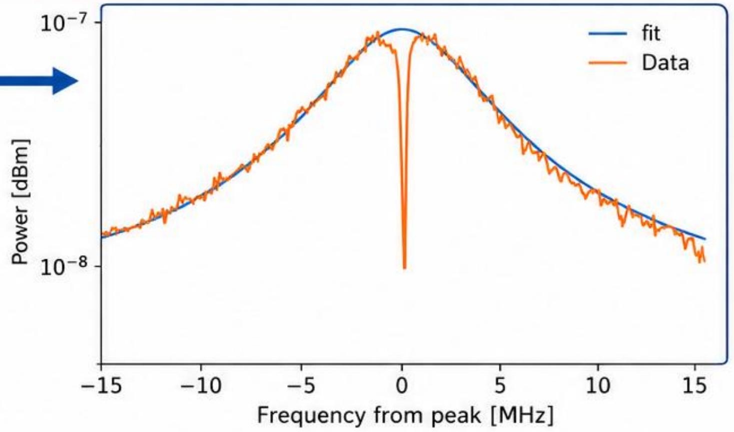

High frequency operation has to cope with large IL that reduces effective gain

TWPA insertion loss

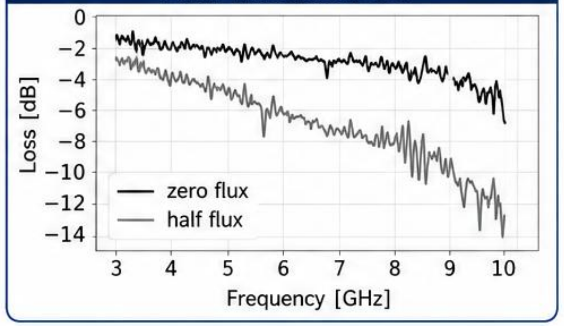

Measured Noise Temperature

T_{sys} = 1.1 K @ 10.2 GHz

T_{sys} = 0.8 K @ 7.9 GHz

-> ~ 2.3 Photons

G. Ruoso, Presented at the STDM Conference, Rome, Italy

QUAX-LNL Haloscope

Run Control

Run steps:

1. Cavity tuning (5 m)
2. TWPA amplifier set ()
3. Measurement of T_{sys} and Gain (2 m)
4. Measurement of f_c, Q_L, Q_0, gain profile (2 m)
5. Short data acquisition with thermal input (2 m)
6. Repeat steps 3-4 (4 m)
7. Long data acquisition with no input (65 m)
8. Repeat steps 3-4 (4 m)
9. Start over

Time for a single point: **80 – 100 minutes**

Slow control

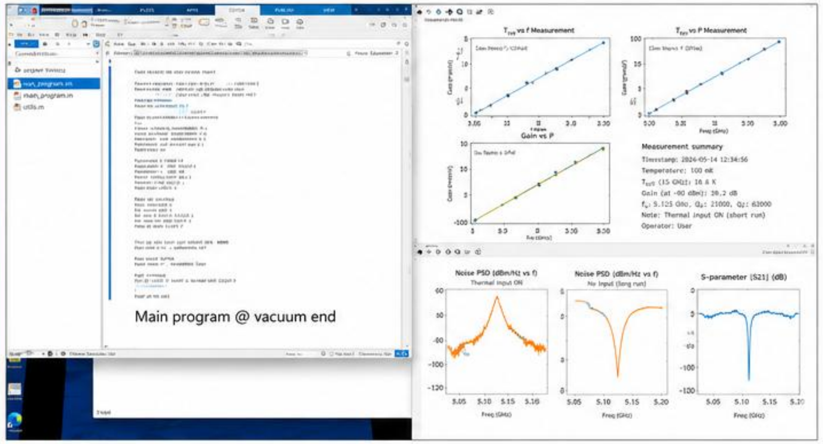

All measured parameters, data and spectra saved to logfiles

Noise Temperature Measurement @ every step

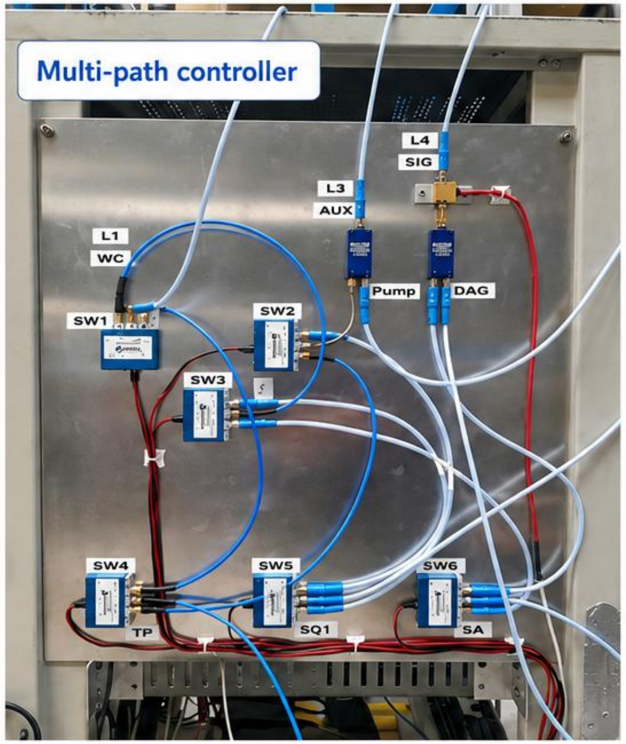

Original idea published in:

A haloscope amplification chain based on a travelling wave parametric amplifier – *Rev. Sci. Instrum.* 2022

G. Ruoso, Presented at the STDM Conference, Rome, Italy

QUAX-LNL Haloscope

Data Acquisition

- 2-channel acquisition (I, Q from Mixer)
- **Sampling rate** = 4.4 MS/s
- Single block length 2^23 = 8 388 608 samples
- Single block length = 1.908 s

- **FFT of each block during acquisition**
- $f_{LO} \sim f_c - 1$ MHz
- Spectral window [f_{LO} – 2.2 MHz, f_{LO} + 2.2 MHz]
- **16384 bins of 268.6 Hz width**

Raw time data and FFTs stored locally during acquisition
Data copied to cloud once per day

ADC control

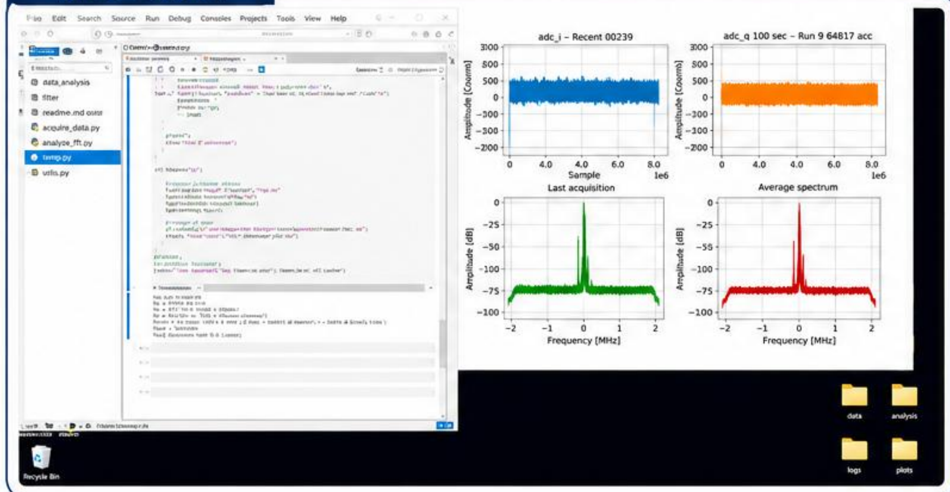

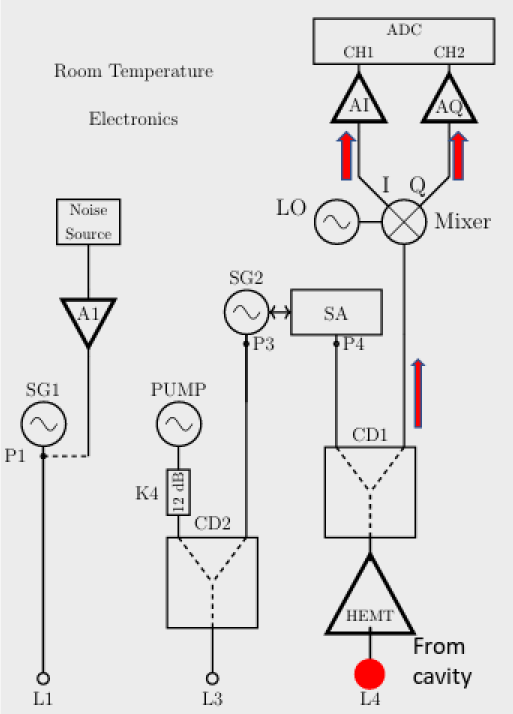

- Data file size 33.6 MByte
- Typical run 65 GByte
- Daily request > 1 TByte
- Total memory storage up to about 20 TByte

G. Ruoso, Presented at the STDM Conference, Rome, Italy

QUAX-LNL Haloscope

QUAX Run 2024

Run summary

- Magnetic field ON
- Cavity frequency f_c = **10.15–10.21 GHz**
- Noise temperature T_{sys} = **1.1–1.5 K**
- Quality factor Q_0 = **60000–80000**
- Antenna coupling β = **1.4–1.8**
- Cavity Volume **V = 1.16 liters**
- Estimated efficiency C_{030} = **0.4**
- Effective field B^2 = **50.89 T^2**
- Axion mass m_a = **44.9 μeV**
- Typical Integration time t_m = **3800 s**

Expected axion power in a 10 kHz window **P_a = 6.0e-24 W**

Expected sensitivity (Dicke) in a 10 kHz window **σ_P = 2.5e-23 W**

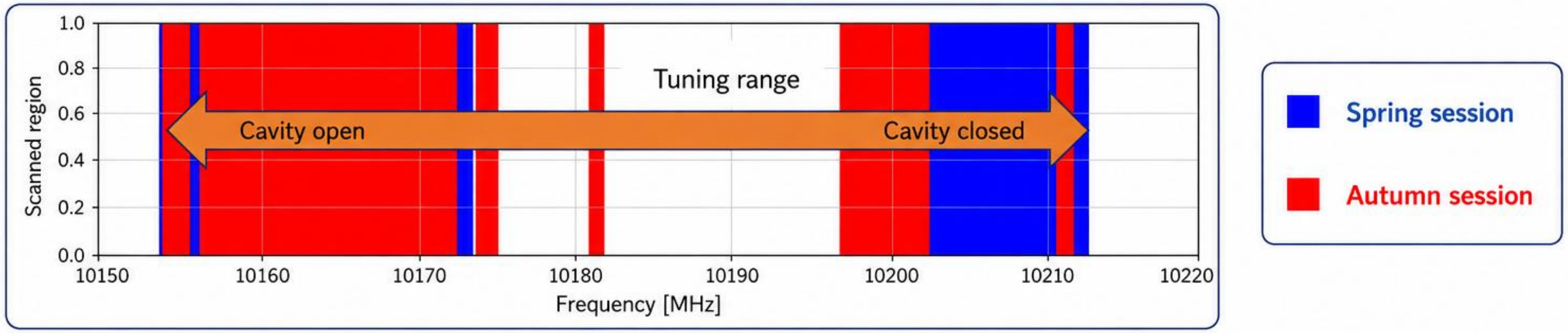

G. Ruoso, Presented at the STDM Conference, Rome, Italy

QUAX-LNL Haloscope

QUAX Run 2024

Spring session

Total run time 3 weeks

2 separate weeks for data taking

May 28th to May 30th - 48 h of field ON

June 11th to June 14th - 90 h of field ON

Autumn session

Total run time 2 weeks

Nov 7th to Nov 13th - 138 h of field ON

Break due to power failure

Nov 19th to Nov 21th - 42 h of field ON

Covered span:
~40 MHz with 225 h vacuum data taking

Maximum tuning: 58.45 MHz

Ratio: 65% of available scan

Duty cycle 50%

Effective scan rate about
100 kHz/hour
2.5 MHz/day

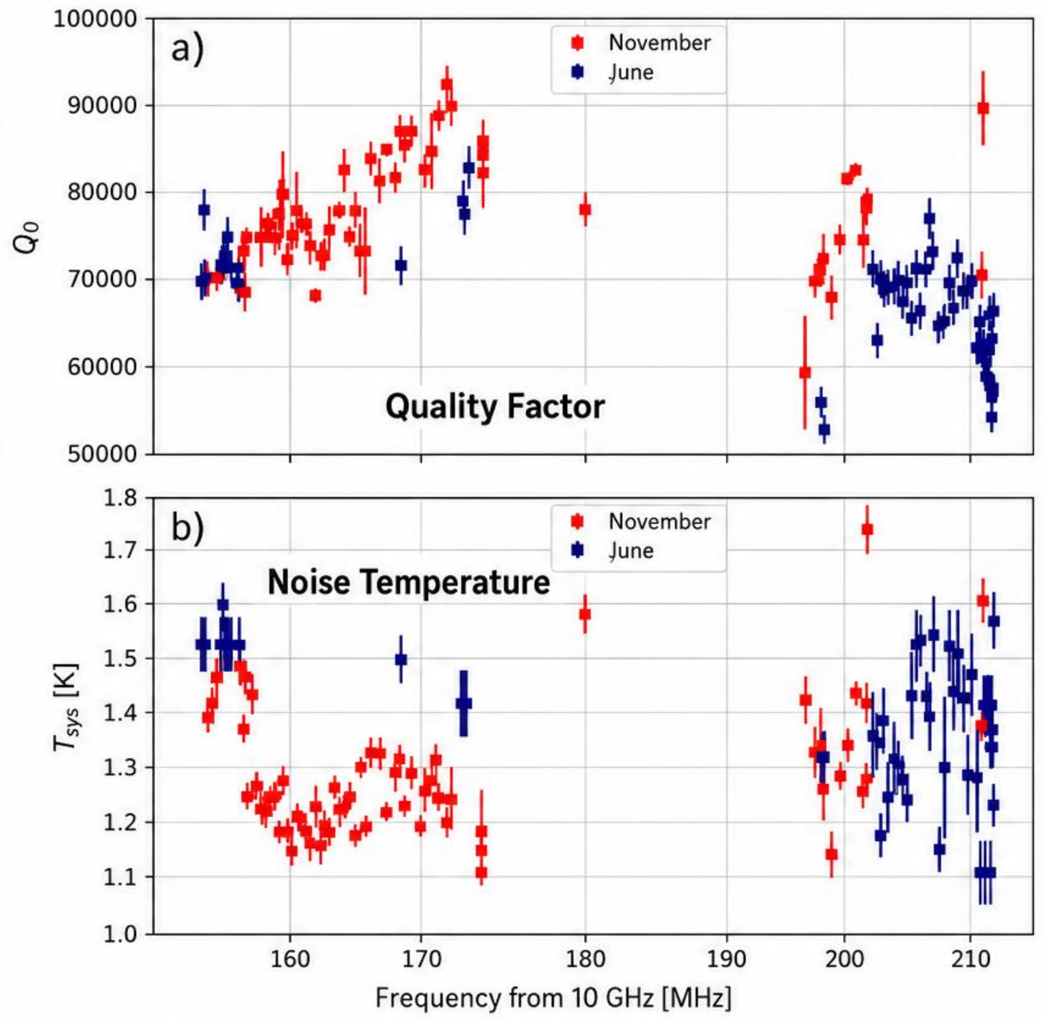

G. Ruoso, Presented at the STDM Conference, Rome, Italy

QUAX-LNL Haloscope

Data Analysis

Parameter evaluation (β, f_c, Q_0, Q_L)

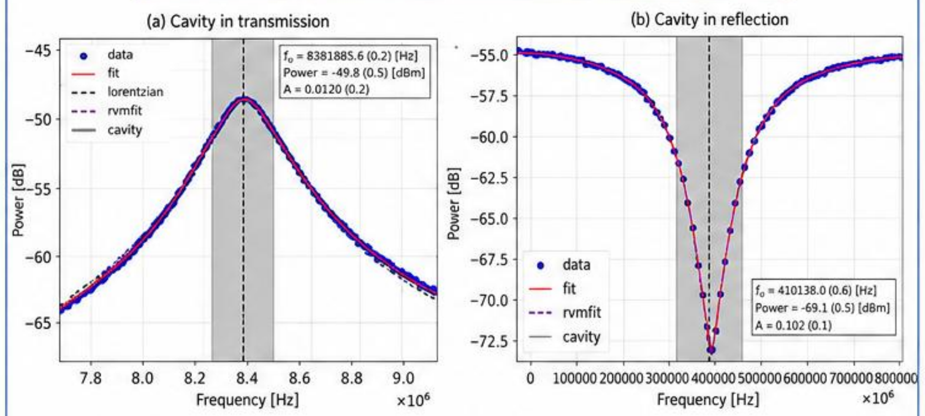

Remove freq-dependent

TWPA

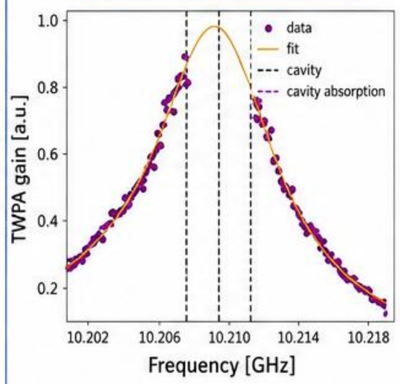

Filters

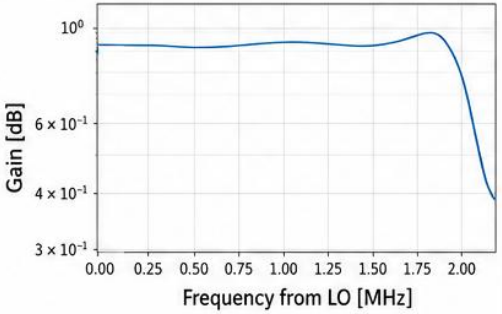

- Average FFT of single frequency steps (bin = 268 Hz)
- Baseline removal with Savitzky Golay filtering
- Monte Carlo simulations to build confidence belts and look for excess power

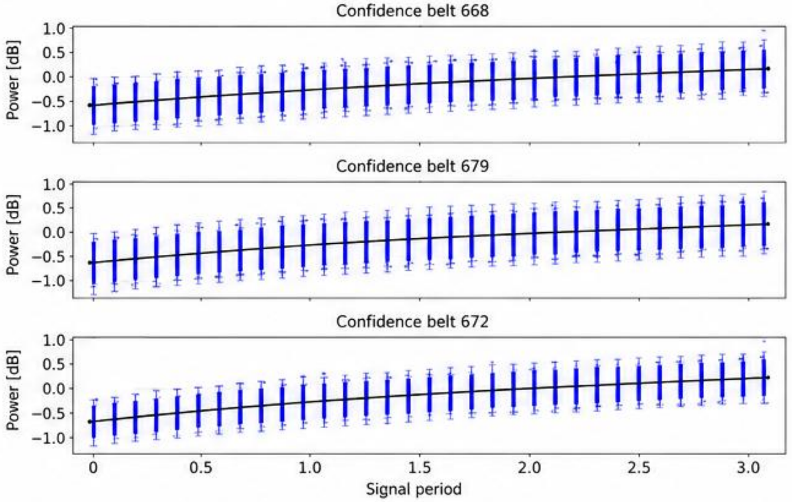

Axion power

$$P^a_{\rm in}(\nu,\nu_a) = g^2_{a\gamma\gamma}\frac{\hbar^3 c^3 \rho_a}{m_a^2}\frac{2\pi\nu_a}{\mu_0}B^2 V C_{030} f_a(\nu,\nu_a)$$

Maxwell-Boltzmann distribution

$$f_a(\nu,\nu_a) = \frac{2}{\sqrt{\pi}}\,\nu\sqrt{\nu-\nu_a}\left(\frac{3}{1.7\nu_a\langle\beta_a^2\rangle}\right)^{3/2} e^{-\frac{3(\nu-\nu_a)}{1.7\nu_a\langle\beta_a^2\rangle}}$$

G. Ruoso, Presented at the STDM Conference, Rome, Italy

QUAX-LNL Haloscope

QUAX Run 2024 Result

No candidate signal have been detected with threshold 4.5 σ

- **Axion-photon limits at 90% C.L.**

PHYSICAL REVIEW LETTERS **135**, 211002 (2025)

Search for Postinflationary QCD Axions with a Quantum-Limited Tunable Microwave Receiver

G. Sardo Infirri,[1,2,*] D. Alesini,[3] C. Braggio,[1,2] G. Cappelli,[4] G. Carugno,[1,2] D. D'Agostino,[3] A. D'Elia,[3] D. Di Gioacchino,[3] R. Di Vora,[6] M. Esposito,[1,2] P. Falferi,[5,8] U. Gambardella,[5] A. Garlidonato,[3] C. Gatti,[3] C. Ligi,[3] G. Lilli,[6] A. Lombardi,[6] G. Maccarrone,[6] D. Maiello,[1,2] A. Ortolan,[5] A. Ranadive,[1,3] A. Rettaroli,[3] N. Roch,[4] S. Tocci,[3] and G. Russo[6,*]

(QUAX Collaboration)

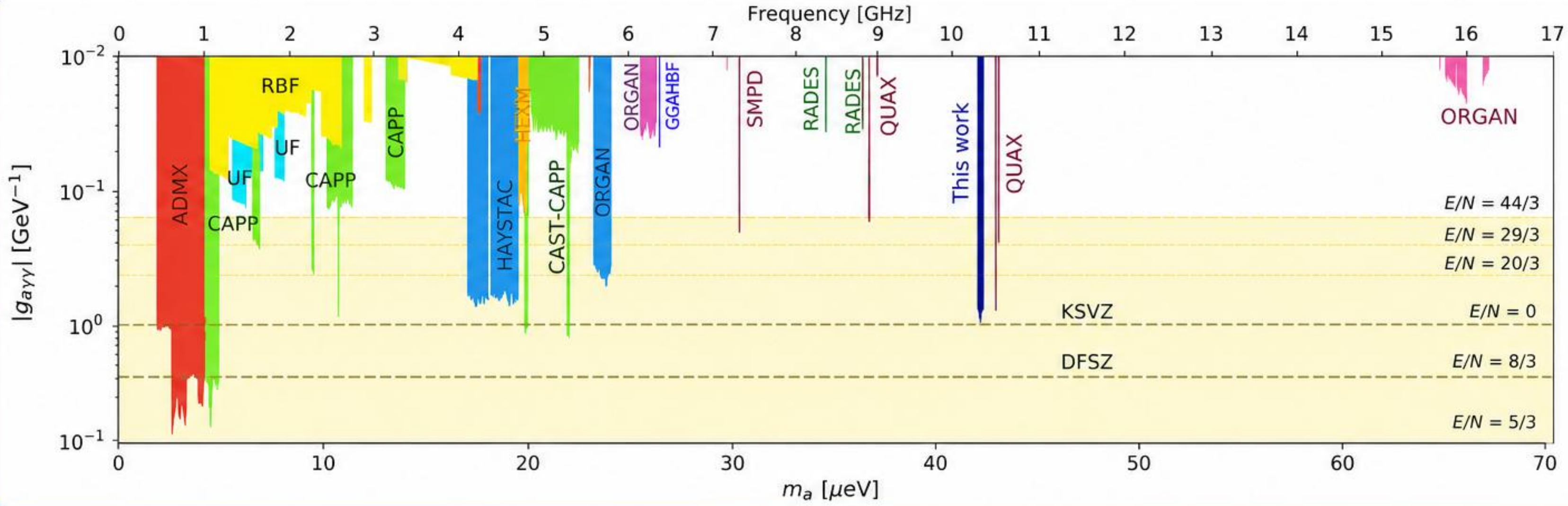

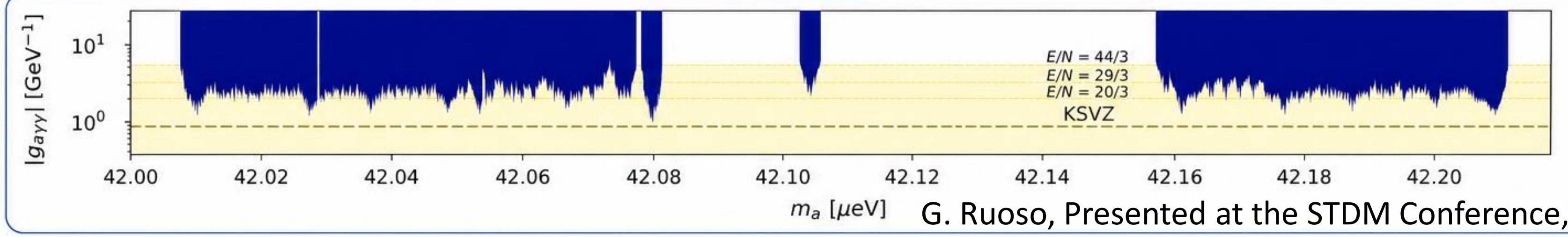

G. Ruoso, Presented at the STDM Conference, Rome, Italy

QUAX-LNL Haloscope

Measurement Sessions 2025-2026

- Major problems with DU unit, reduced machine availability
  → **Problems now solved**
- No changes on the RF hardware
- Improvement on tuning mechanism to exploit full cavity range
- Improvements on the RF and acquisition system to employ almost full **automation**

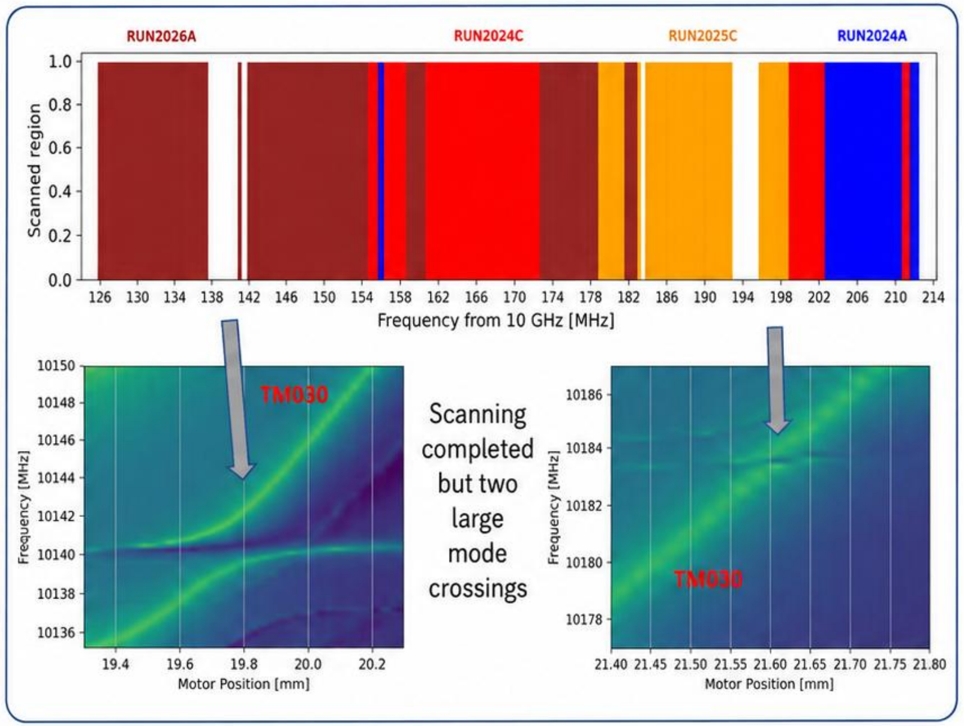

2025C session

Total run time 8 days

Nov 13th to Nov 17th - 92 h of field ON
Scanned about 15 MHz

2026A session

Total run time 11 days

April 28th to May 6th - 188 h of field ON
Scanned about 34 MHz

Covered span 2025 - 2026:
~49 MHz with 280 h magnetic field ON

Effective scan rate about
180 kHz/hour
4.2 MHz/day

Data analysis on the way !

G. Ruoso, Presented at the STDM Conference, Rome, Italy

QUAX-LNL Haloscope

Future Plan

- Data analysis and check for re-scanning with current cavity
- **Install new cavity with larger tuning and increased Q factor**

SAMEK 3G

(Phoenician: Pillar)

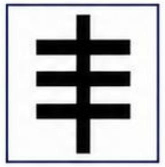

- New endcaps – two sliding parts
- No rf sliding contacts
- New aperture mechanism

Preliminary results:

tuning range 170 MHz (10.04 – 10.21 GHz)

with Q0 ~ 100 000 – 130 000

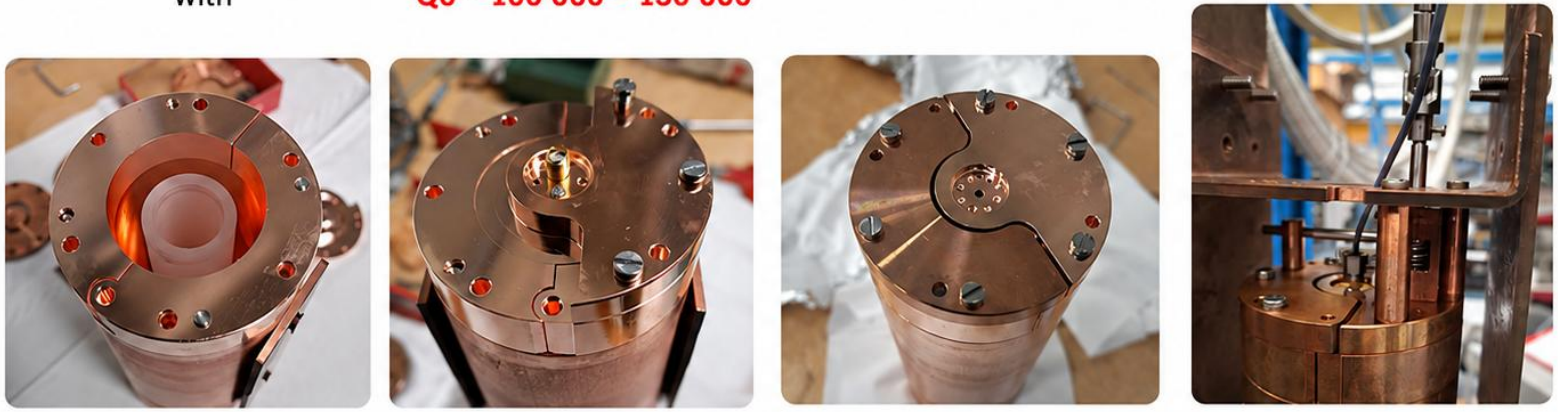

G. Ruoso, Presented at the STDM Conference, Rome, Italy

QUAX-LNL Haloscope

Future Plan

- Short prototype for testing
- Length = 243.4 mm
- Inner diameter 60.5 mm
- Sapphire from Lithuania
- Science mode TM030

Tested @ 4 K

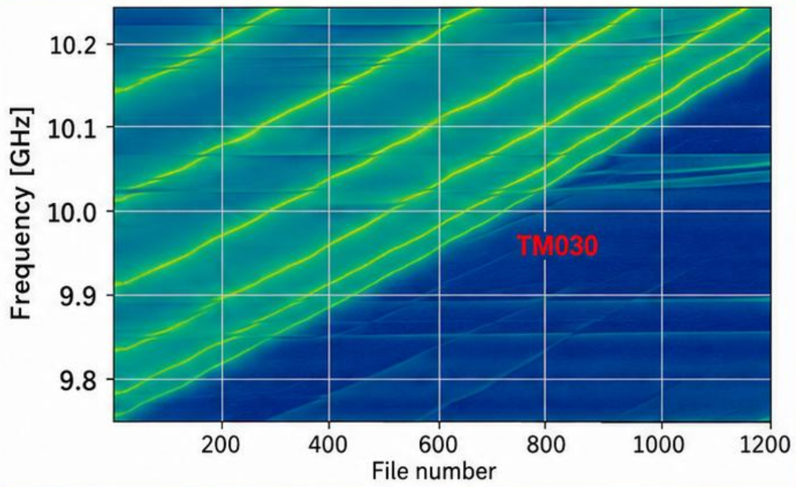

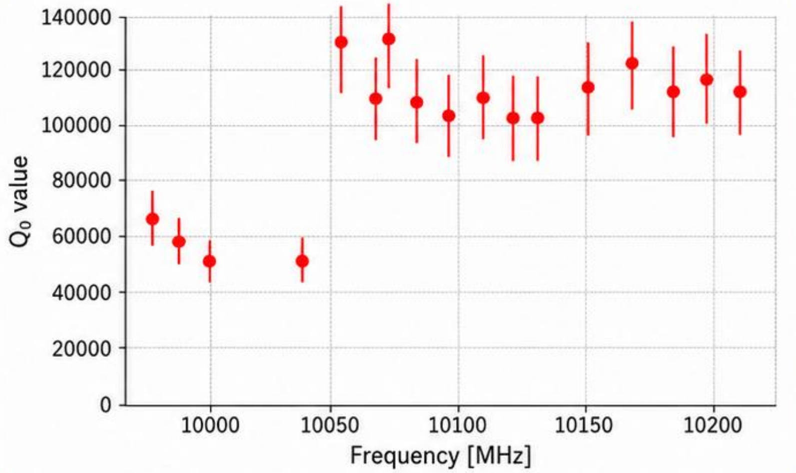

G. Ruoso, Presented at the STDM Conference, Rome, Italy

QUAX-LNL Haloscope

Future Plan

1 Installation of a 14 T magnet

Expected summer 2026

JASTEC SUPERCONDUCTOR

Model	JMTA-14T103
Coil configuration	Solenoid coil
Maximum central field	14 Tesla
Free bore diameter	103 mm
Outer diameter of the solenoid	400 mm excluding protrusion (tentative)
Total height of the solenoid	500 mm excluding protrusion (tentative)
Total weight (approximately)	250 kg (tentative)
Field direction	Vertical two-way
Operating current (nominal)	185 A (tentative)
Inductance	64 Henries (tentative)
Maximum sweep rate	14 Tesla / 60 minutes (tentative)
Field homogeneity (designed value)	More than 9 Tesla in a cylindrical area of 60mm diameter and 420 mm height

Photo 1 Appearance of JMTA-14T103.

2 Single Photon Microwave Detector (SMPD)

Help of Quantronics Group Paris

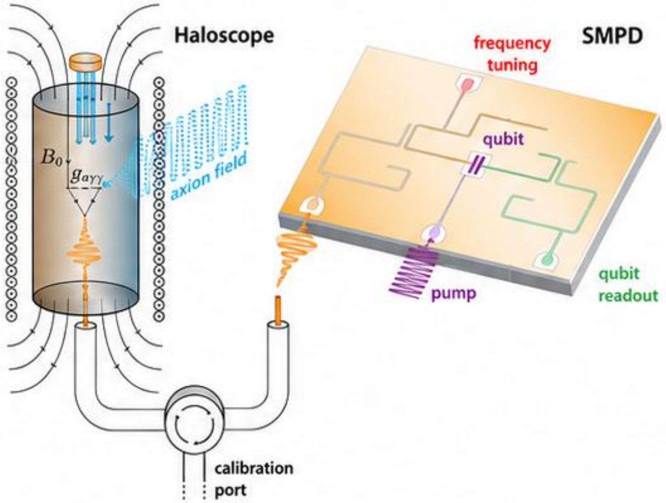

3 New TWPA

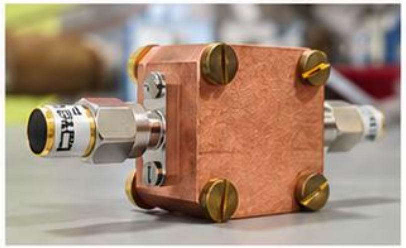

amplifier from Grenoble optimized for 10 – 11 GHz band

4 Installation of new cryogenic system

- Wet assembly for magnet
- Dry unit for cavity and rf detection

This will allow for longer and safer operation.

G. Ruoso, Presented at the STDM Conference, Rome, Italy

QUAX-LNL Haloscope

Future Plan

Single Microwave Photon Detector Readout

Beyond Standard Quantum Limit

1. SQL Linear Amplifier (measures amplitude)

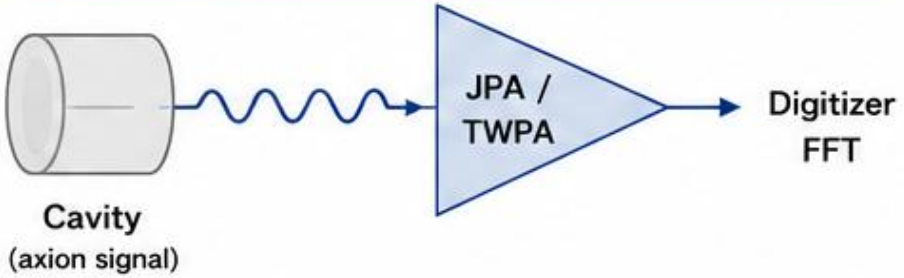

What is measured?
Field quadratures X and P (amplitude & phase)

Heisenberg uncertainty: $\Delta X \Delta P \geq 1/2$
⇒ Vacuum fluctuations ($1/2$ photon) are always added.

Noise (SQL)

Noise-equivalent power:

$$P_{\mathrm{SQL}} = h\nu$$

$$\mathrm{SNR}_{\mathrm{SQL}} = \frac{P_a}{h\nu}\sqrt{\frac{t}{\Delta\nu_a}}$$

P_a : axion signal power, $\Delta\nu_a$: axion linewidth, t : integration time

2. SMPD (measures photon number)

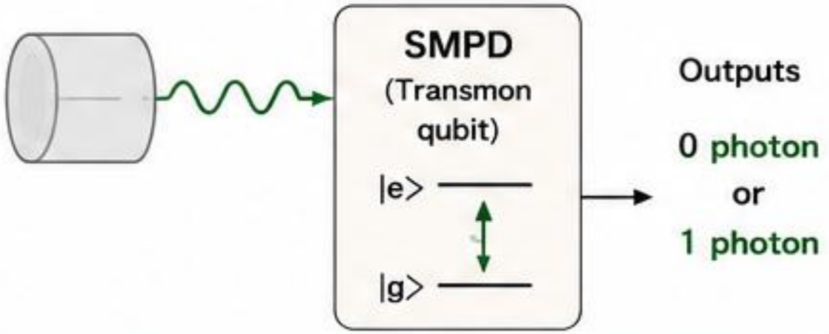

What is measured?
Photon number $n = a^\dagger a$ (YES / NO)

Noise (SMPD)

Counts obey Poisson statistics.

Total count rate: $\Gamma_{\mathrm{tot}} = \Gamma_s + \Gamma_{\mathrm{dc}}$

(Γ_s: signal; Γ_{dc}: dark counts (thermal + intrinsic))

$$\mathrm{SNR}_{\mathrm{SMPD}} \approx \frac{\Gamma_s}{\sqrt{\Gamma_{\mathrm{dc}}}}\sqrt{t} \quad \text{(weak-signal limit)}$$

Single Microwave Photon Detector Readout

Beyond Standard Quantum Limit

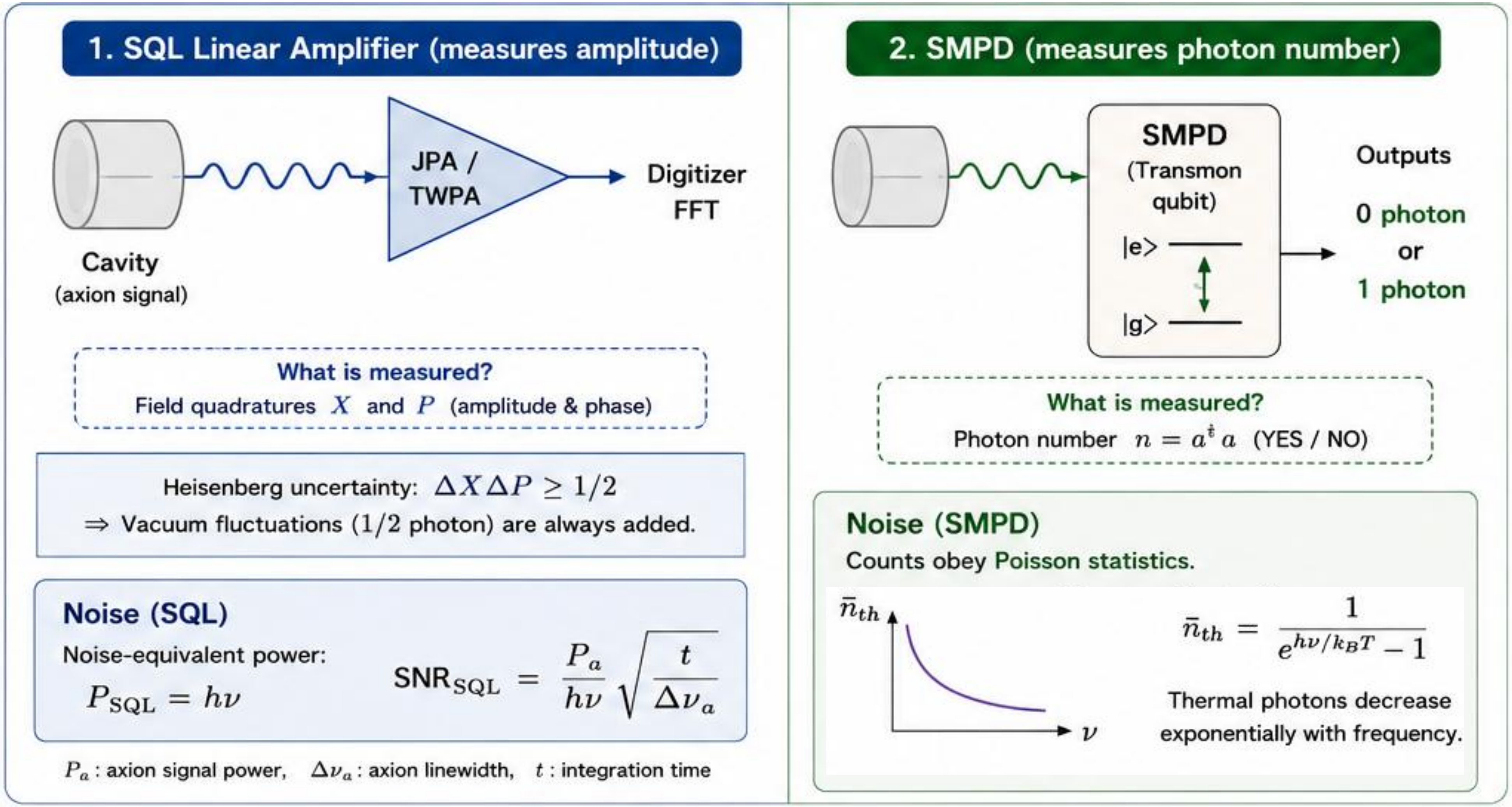

Single Microwave Photon Detector Readout

Working Principle

Detector principle

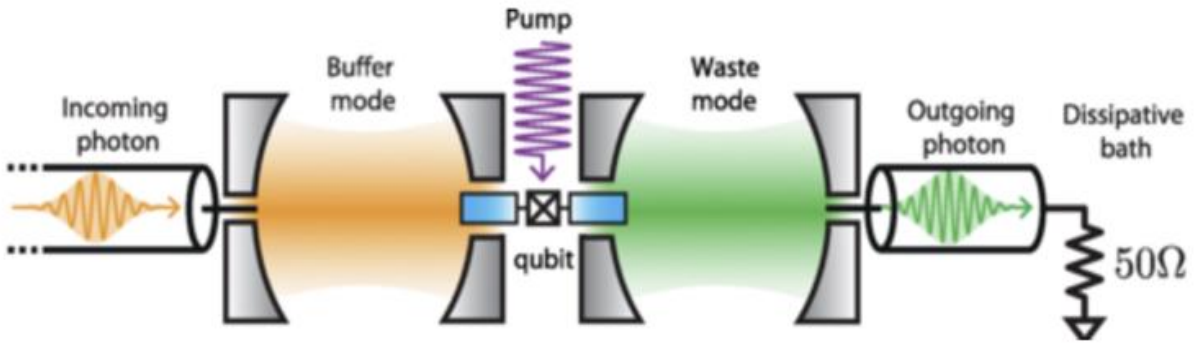

A pump-activated four-wave mixing interaction **coherently converts a buffer photon into a qubit excitation** while emitting a photon into the waste mode.

4WM resonance condition

$$\omega_b + \omega_p = \omega_q + \omega_w - \chi_w$$

(χ_w : anharmonicity of the waste mode)

- ω_b buffer mode frequency
- ω_p pump frequency
- ω_q qubit frequency
- ω_w waste mode frequency

Cyclic operation of one detection cycle

The detector operates in repeated **detection–readout–reset** cycles.

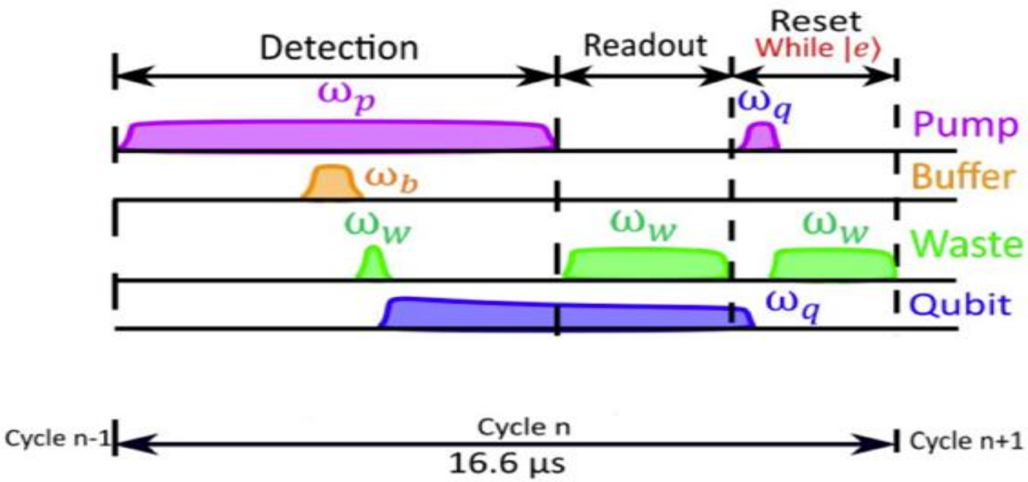

Outcome of each cycle:

- No click ($|g\rangle$)
- **Click** ($|e\rangle$)

Single Microwave Photon Detector Readout

Working Principle

Detector principle

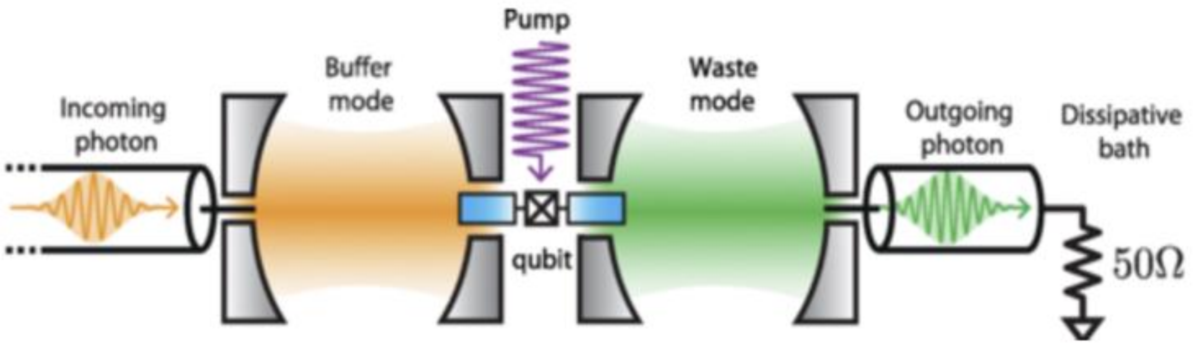

Phys. Rev. X 10, 021038 (2020) ← 1.3 counts/ms
Nature **600**, 434–438 (2021) ← spin fluorescence detection
Nature **619**, 276–281 (2023) ← single spin flip
Phys. Rev. Appl. 21, 014043 (2024) ← 85 counts/s

more at https://iramis.cea.fr/en/spec/gq/

Cyclic operation of one detection cycle

The detector operates in repeated detection–readout–reset cycles.

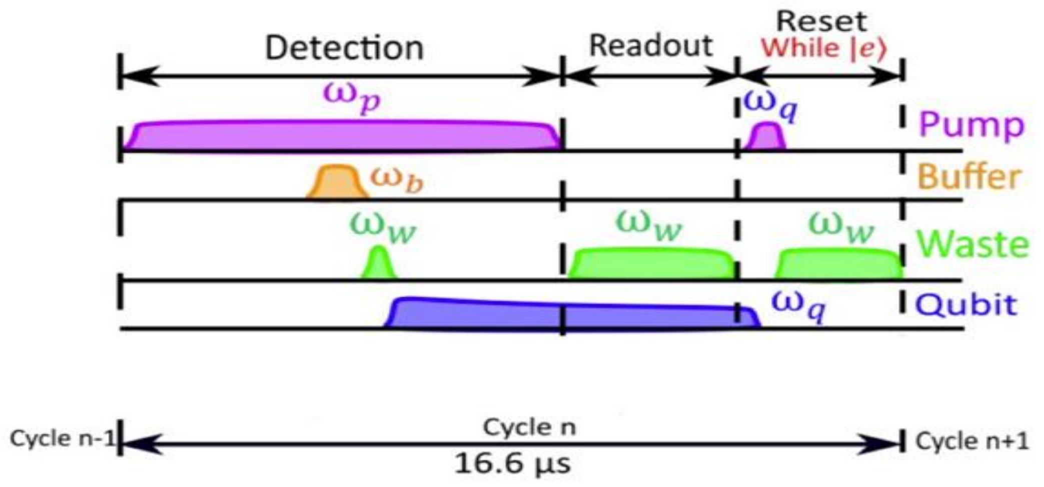

Outcome of each cycle: No click ($|g\rangle$) Click ($|e\rangle$)

Single Microwave Photon Detector Readout

Pathfinder

- a **transmon qubit-based** single microwave photon detector (SMPD) is used to readout the cavity mode
- TWPA for dispersive readout of the qubit state
- hybrid (normal-superconducting) cavity TM_{010} at 7.37 GHz **tunable** by a triplet of rods $Q_0 = 9 \times 10^5$ at 2 T-field
- T=14 mK @ fridge Quantronics lab (CEA, Saclay)

→ investigated the background, and set a limit to $g_{a\gamma\gamma}$ [0.5 MHz band] **X20 compared to SQL**

see also: Kuo *et al* Phys. Rev. D 111, 123018 (2025)

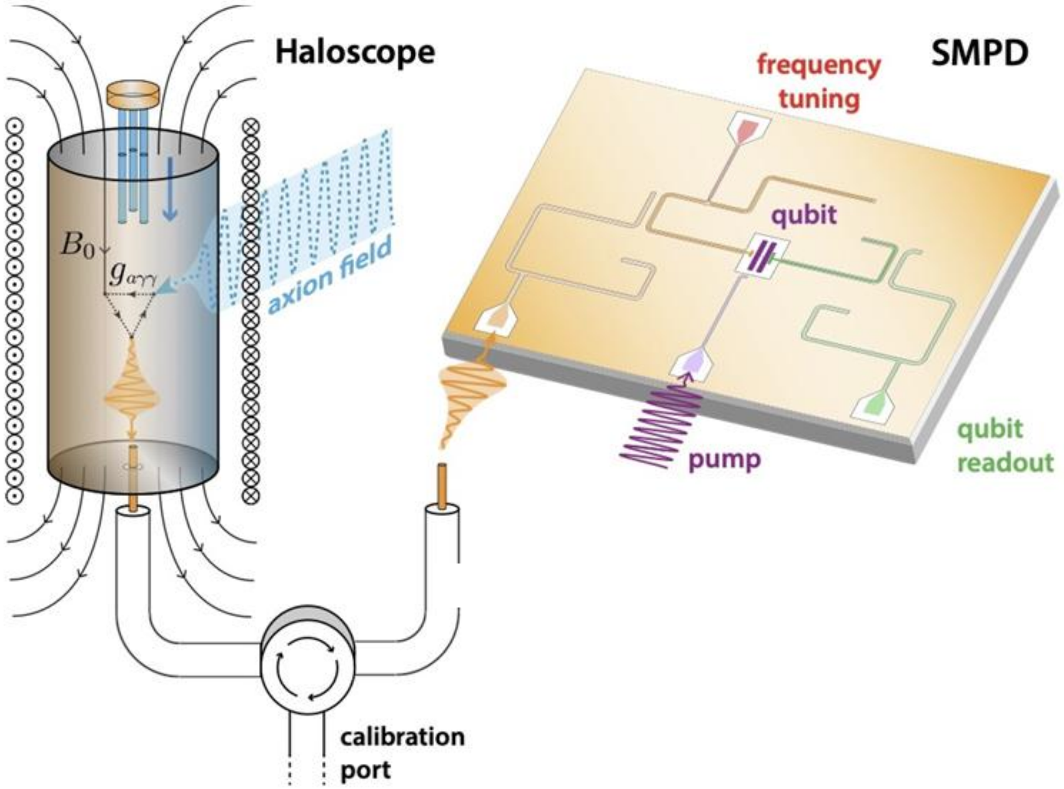

Phys. Rev. X 15, 021031 (2025)

C. Braggio, Presented at the STDM Conference, Rome, Italy

Single Microwave Photon Detector Readout

Pathfinder

C. Braggio, Presented at the STDM Conference, Rome, Italy

- a **transmon-based** single microwave photon detector (SMPD) is used to readout the cavity mode
- TWPA for dispersive readout of the qubit state
- hybrid (normal-superconducting) cavity TM_{010} at 7.37 GHz **tunable** by a triplet of rods $Q_0 = 9 \times 10^5$ at 2 T-field
- T=14 mK @ fridge Quantronics lab (CEA, Saclay)

→ investigated the background, and set a limit to $g_{a\gamma\gamma}$ [0.5 MHz band] **X20 compared to SQL**

see also: Kuo *et al* Phys. Rev. D 111, 123018 (2025)

Single Microwave Photon Detector Readout

Background Limited Search: Dark Counts

C. Braggio, Presented at the STDM Conference, Rome, Italy

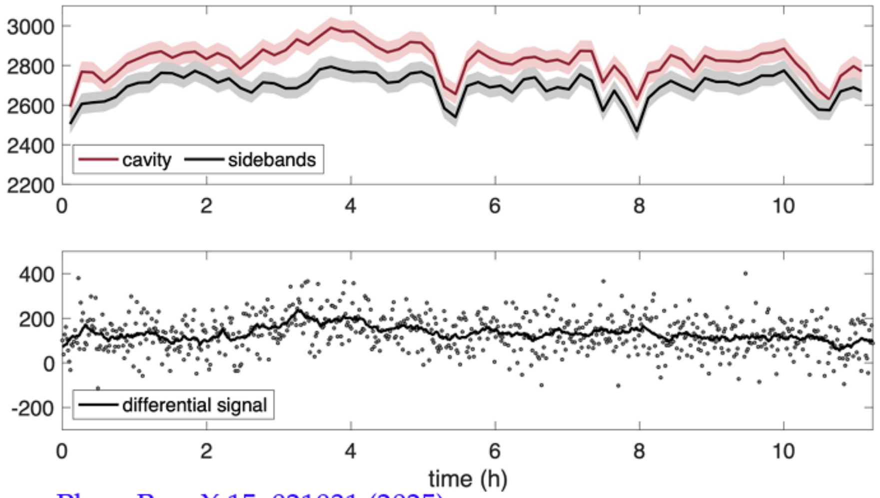

Phys. Rev. X 15, 021031 (2025)

- counts at $\omega_b = \omega_c$ registered in 28.6 s $\iff$ **average dark count rate** $\alpha \sim 90$ **counts/s**
- **excess** at $\omega_c \leftrightarrow$ the cavity sits at a slightly higher te (few mK)
- both the counts at resonance and on sidebands $\omega_b = \omega_c \pm 1, 2\,\text{MHz}$ vary **beyond statistical uncert** expected for poissonian counts

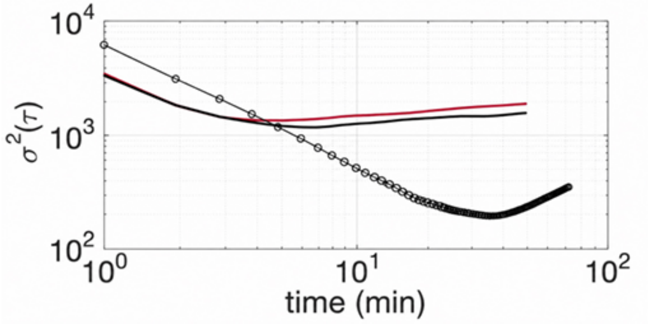

Allan variance $\rightarrow$ max integ. time $\sim$ 10 min.

$\rightarrow$ $\alpha = \alpha_q + \alpha_{4WM} + \alpha_{th}$, where $\alpha_{th} \propto \bar{n}_{th} = \frac{1}{e^{h\nu/kT}-1}$ finite flux of *thermal* photons at the SMPD input

Single Microwave Photon Detector Readout

New Generation SMPD in Our Lab

C. Braggio, Presented at the STDM Conference, Rome, Italy

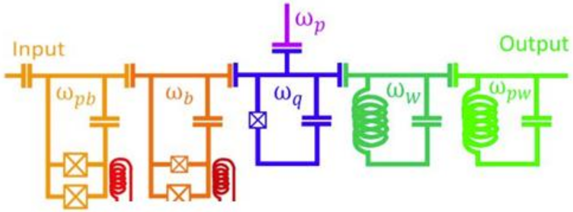

→ Purcell resonator for **tuning buffer bandwidth**

→ DC flux lines for tuning ω_{pb} and ω_b

$$\alpha_{\rm th} = \frac{\bar{n}_{{\rm th},b}\, \eta_{\rm SMPD}(\omega_b)\, \kappa_d}{4}$$

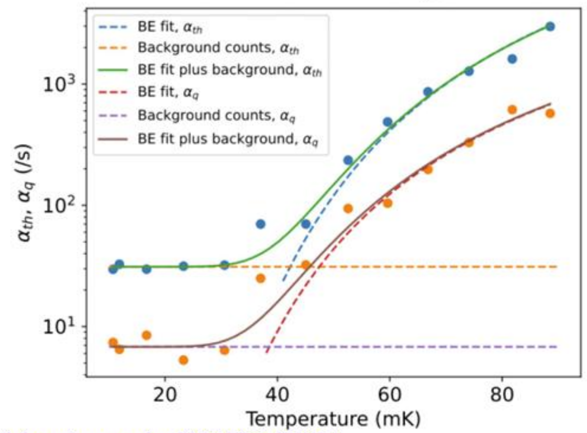

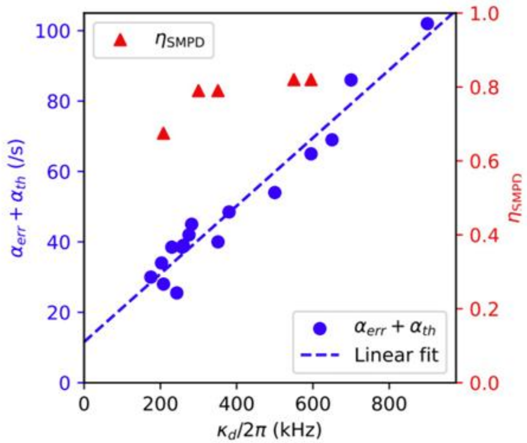

https://arxiv.org/pdf/2501.07354

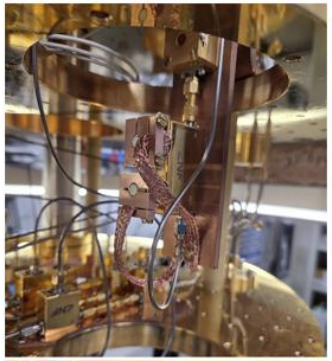

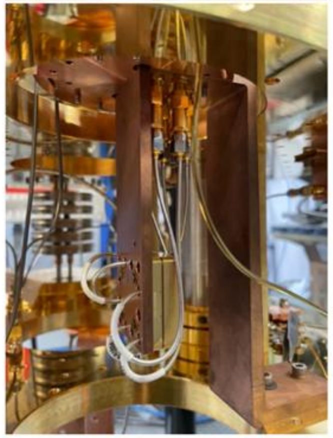

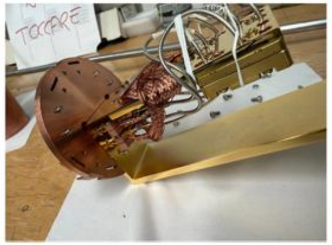

Single Microwave Photon Detector Readout

Experimental Apparatus

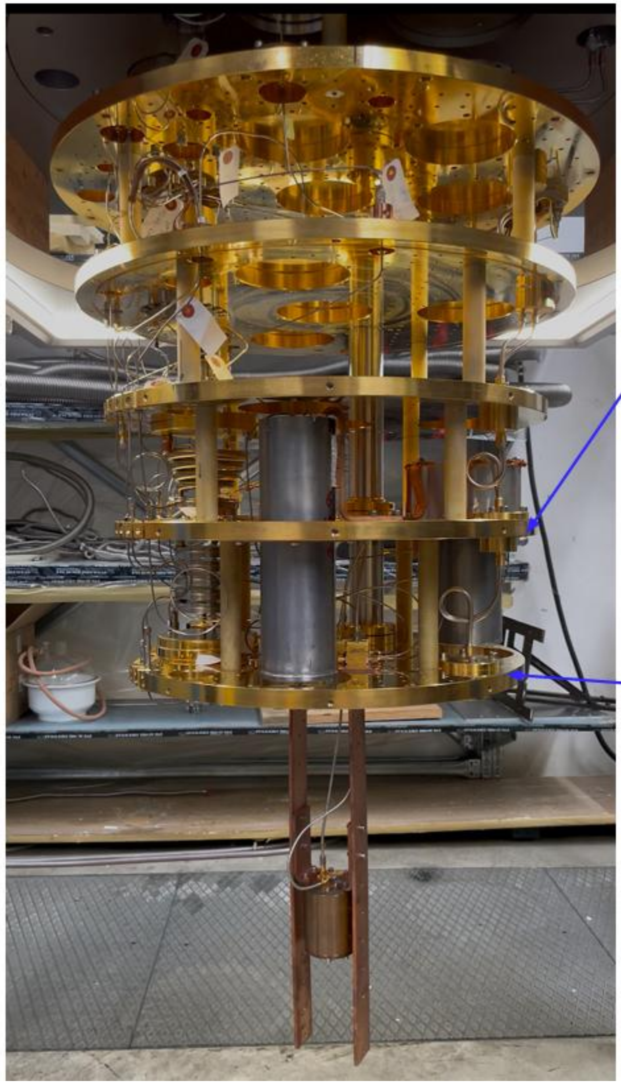

inside of SMPD box

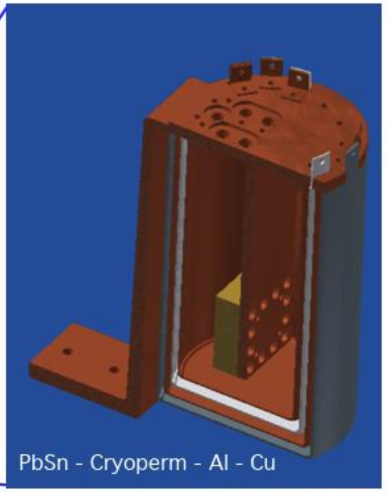

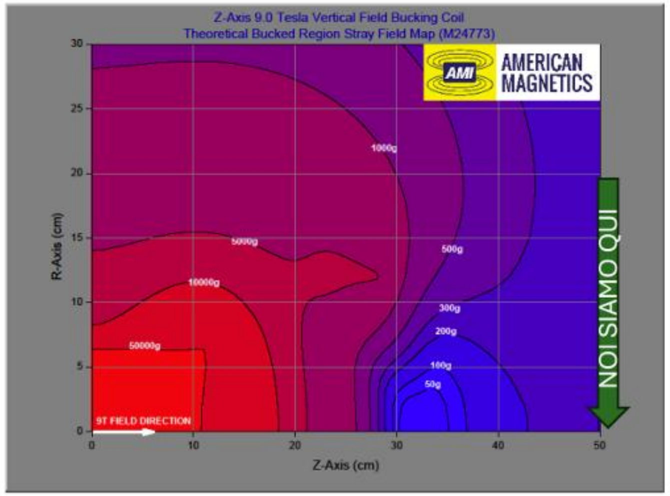

C. Braggio, Presented at the STDM Conference, Rome, Italy

Single Microwave Photon Detector Readout

Experimental Apparatus

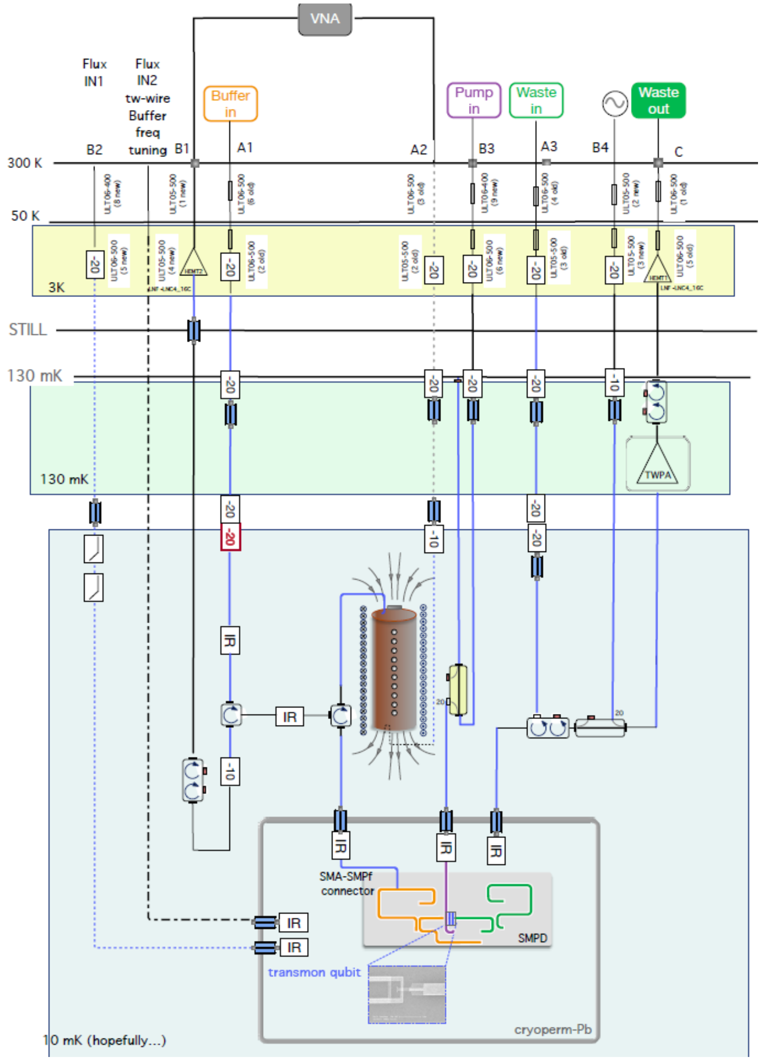

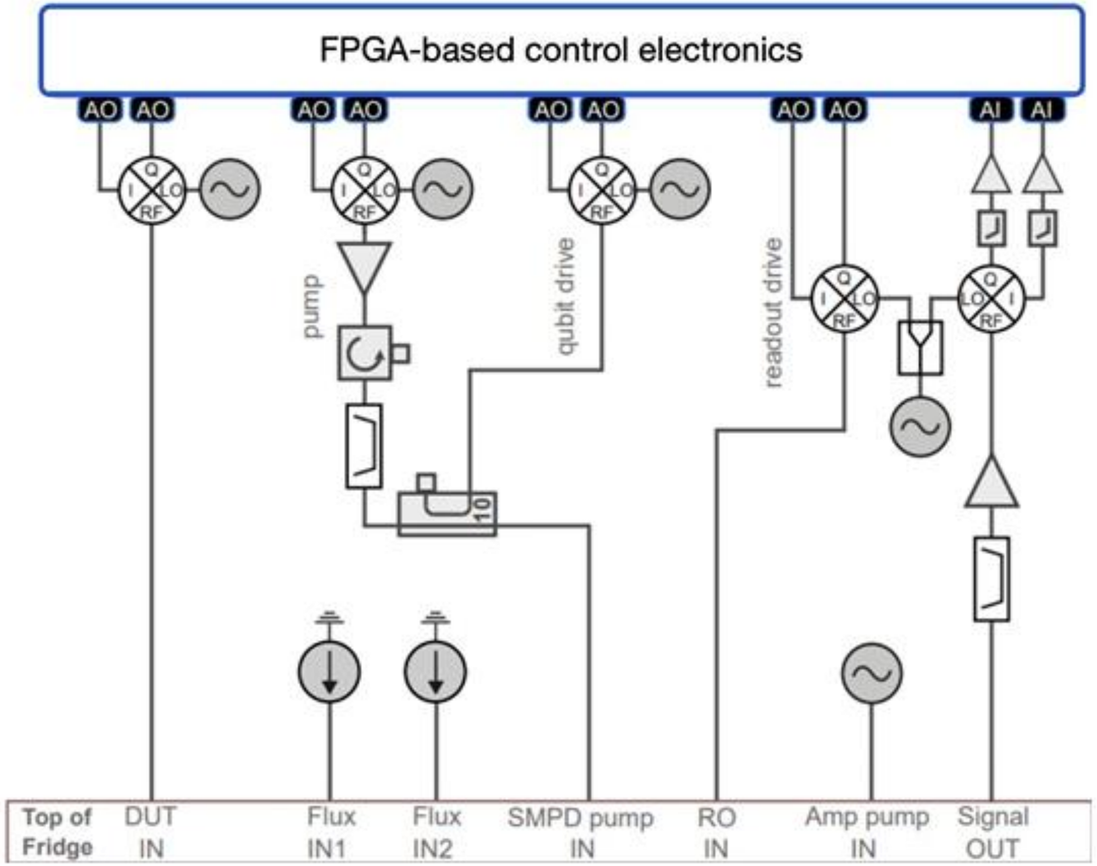

Single Microwave Photon Detector Readout

Qubit Characterization & Photon Counting with 4 Wave Mixing

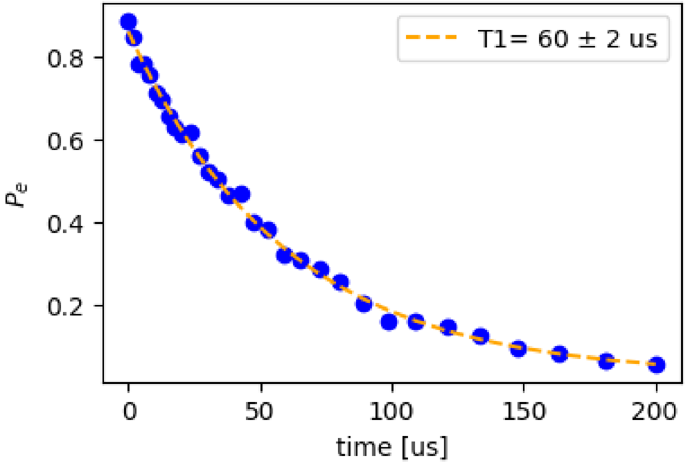

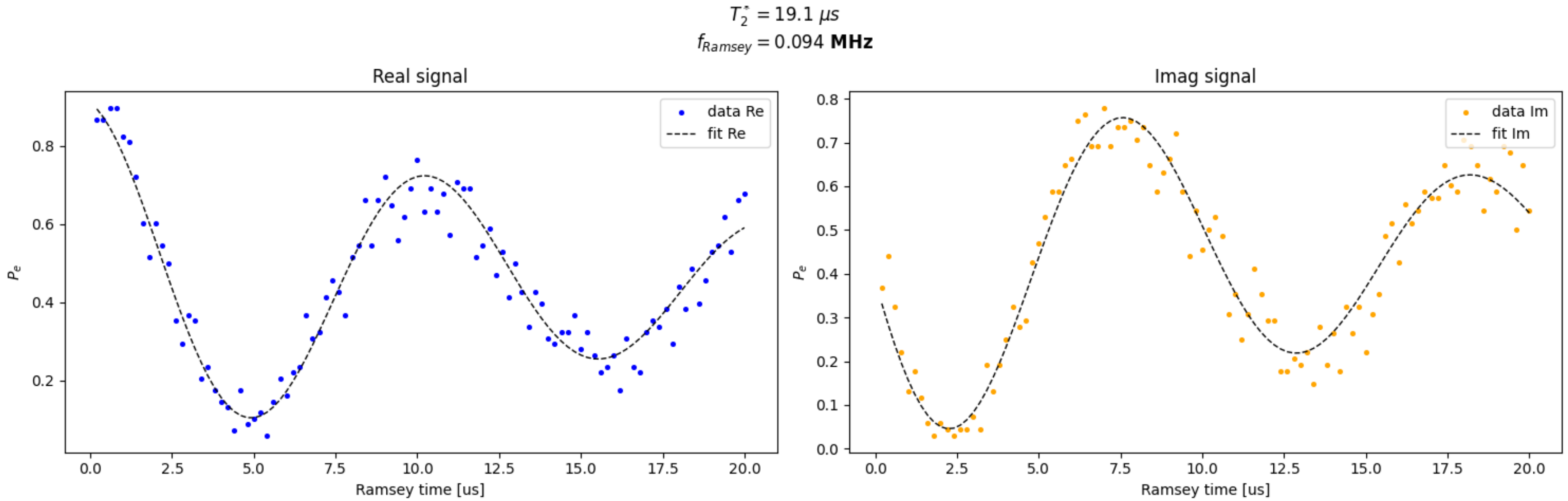

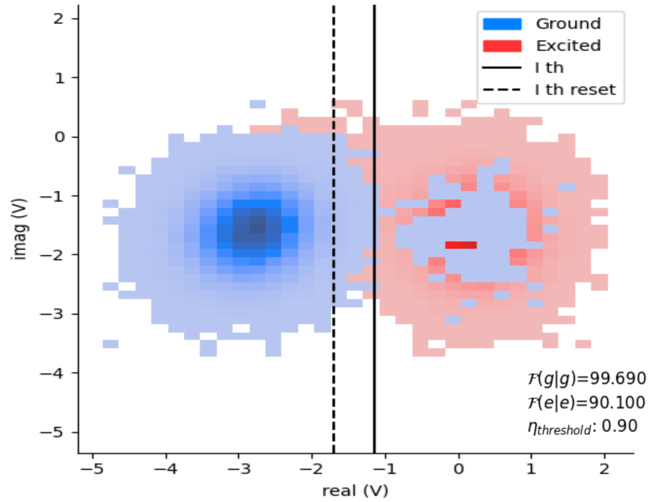

VNA: TWPA optimization, buffer/waste resonator response

FPGA-based Qubit Measurement : T1, T2*, T2Echo, Single-Shot, Qubit Reset

Photon Counting

(1) Calibrate Photon Flux (Stark-Shift)

(2) Four-Wave Mixing Calibration (pump amplitude, frequency & detuning)

(3) Buffer Detection Bandwidth

(4) Photon Counting with Cyclic Sequence (efficiency & dark count)

Single Microwave Photon Detector Readout

Qubit Characterization & Photon Counting with 4 Wave Mixing

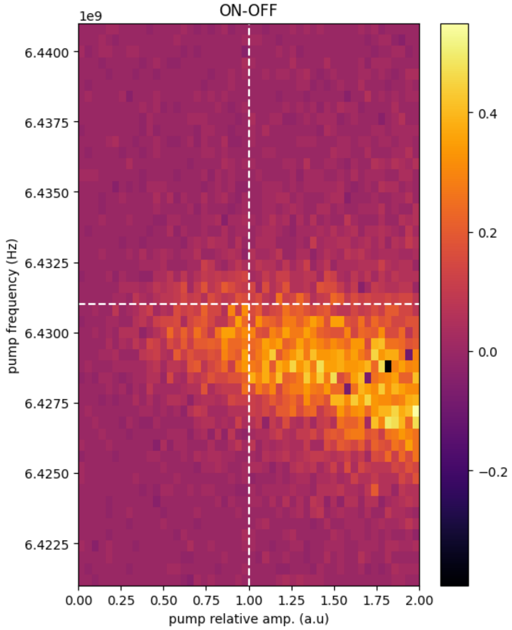

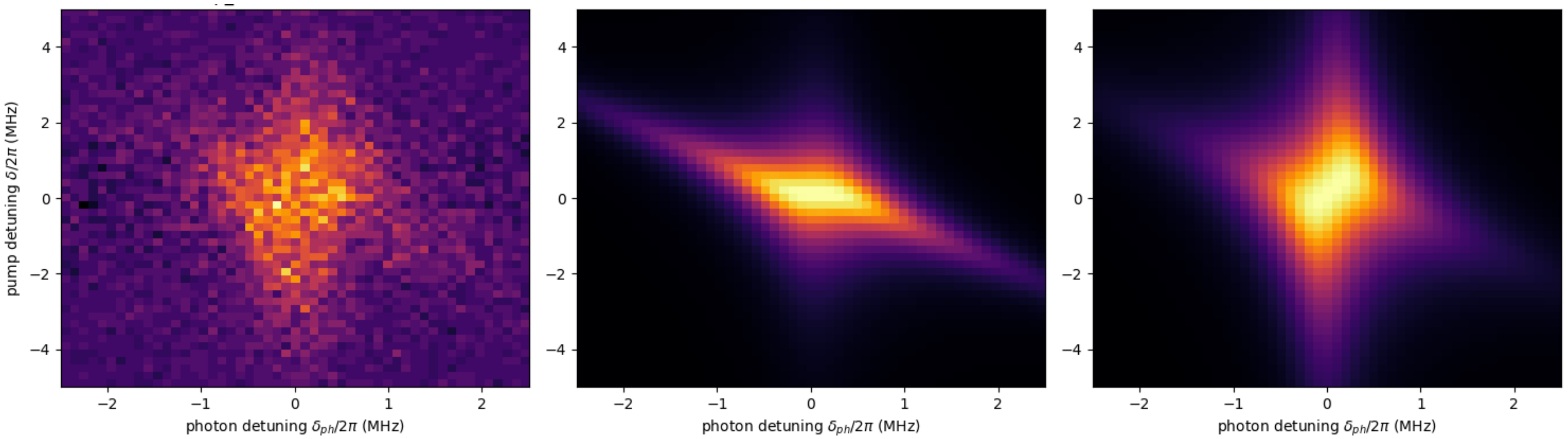

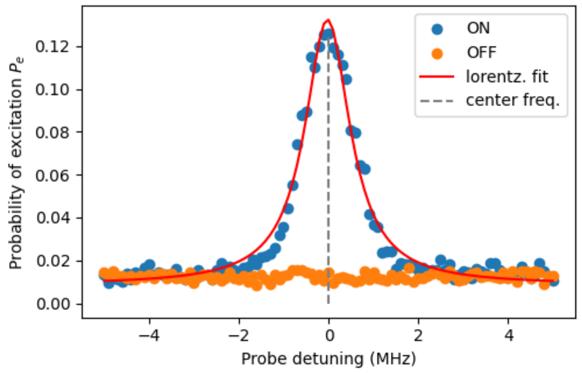

VNA: TWPA optimization, buffer/waste resonator response

FPGA-based Qubit Measurement : T1, T2*, T2Echo, Single-Shot, Qubit Reset

Photon Counting

(1) Calibrate Photon Flux (Stark-Shift)

(2) Four-Wave Mixing Calibration (pump amplitude, frequency & detuning)

(3) Buffer Detection Bandwidth

(4) Photon Counting with Cyclic Sequence (efficiency & dark count)

Single Microwave Photon Detector Readout

New Generation SMPD in Our Lab

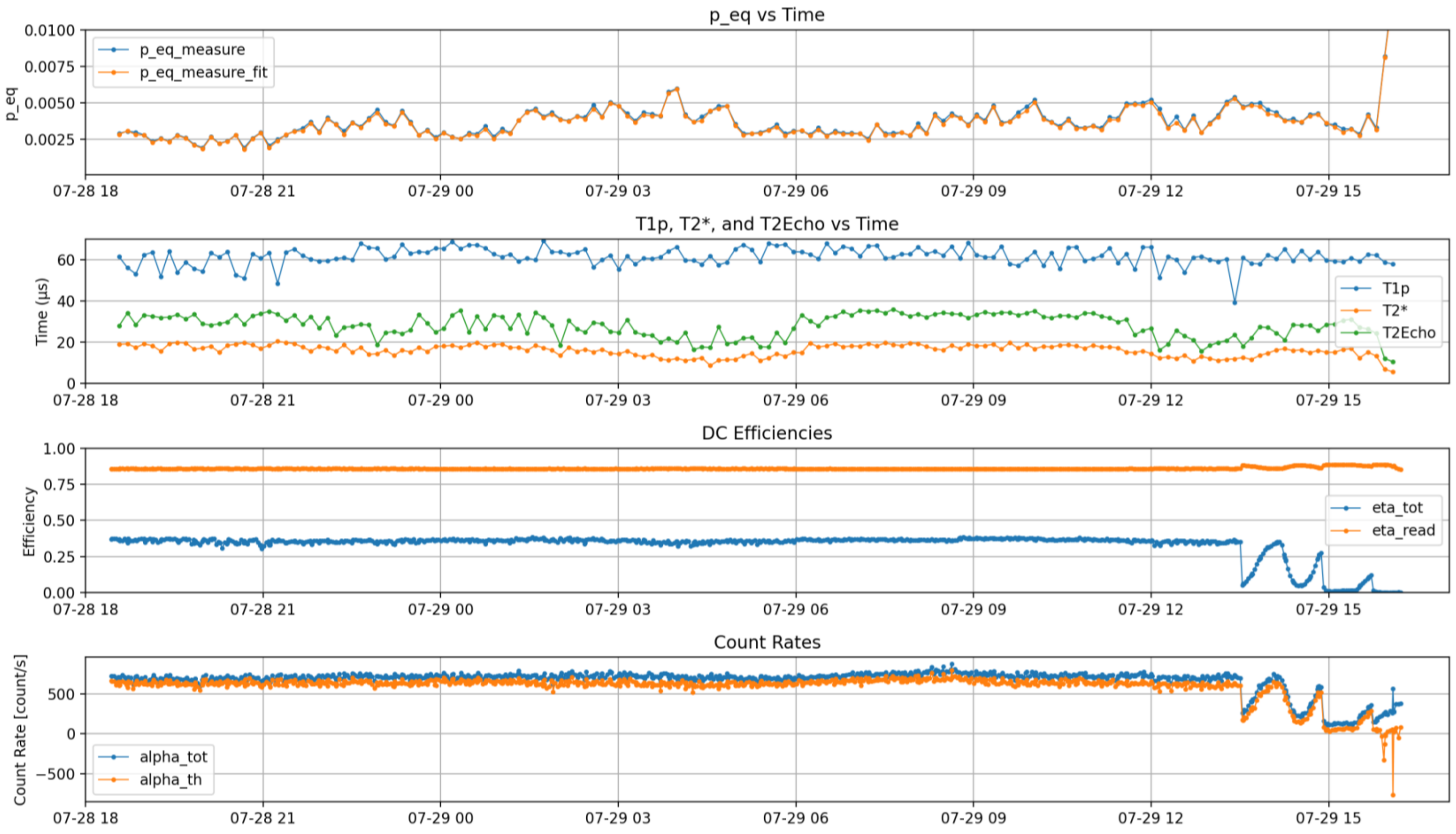

D. Ahn, INFN-SQMS PostDoc (formerly at CAPP)
G. Sardo Infirri, UniPD PhD student

SQUID Readout

Motivation: kHz Axion Dark Matter Detection

https://cajohare.github.io/AxionLimits/

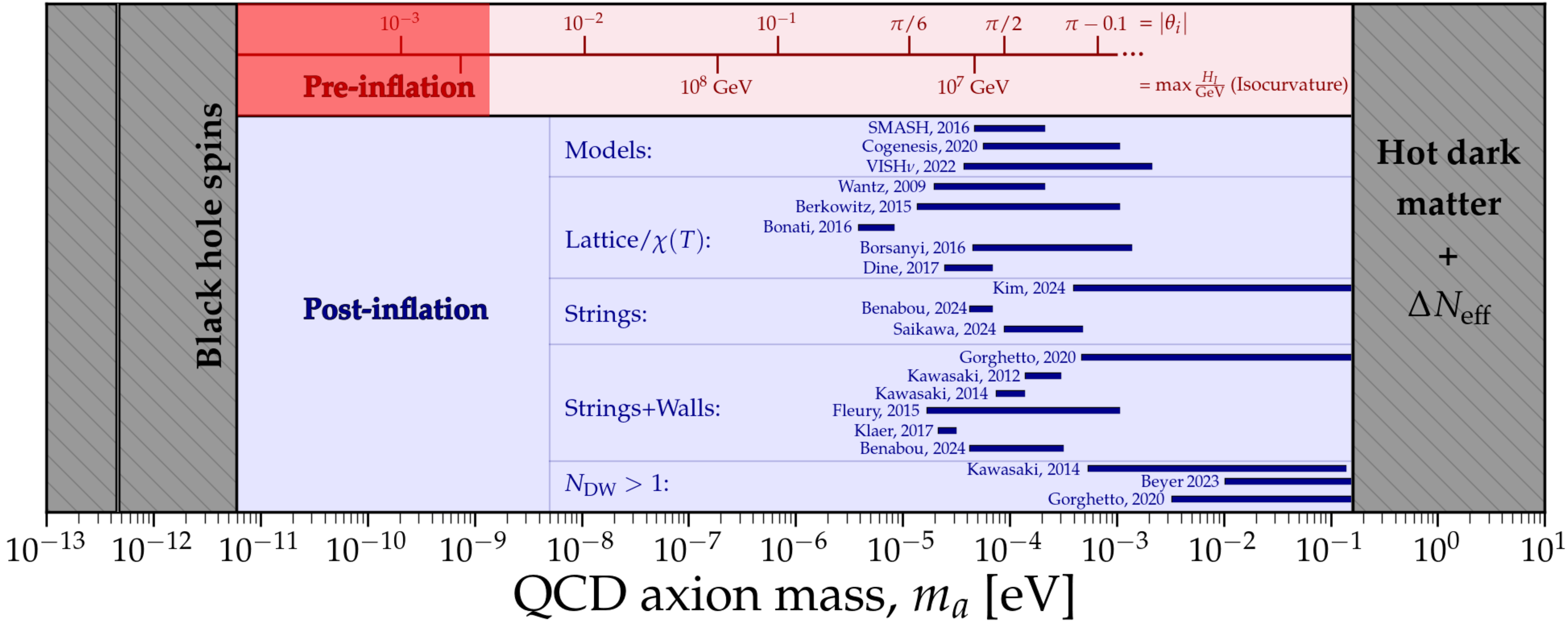

SQUID Readout

Motivation: Gravitational Wave Detection

Extend Detection Frequency O(10 kHz)

PHYSICAL REVIEW D 93, 112004 (2016)

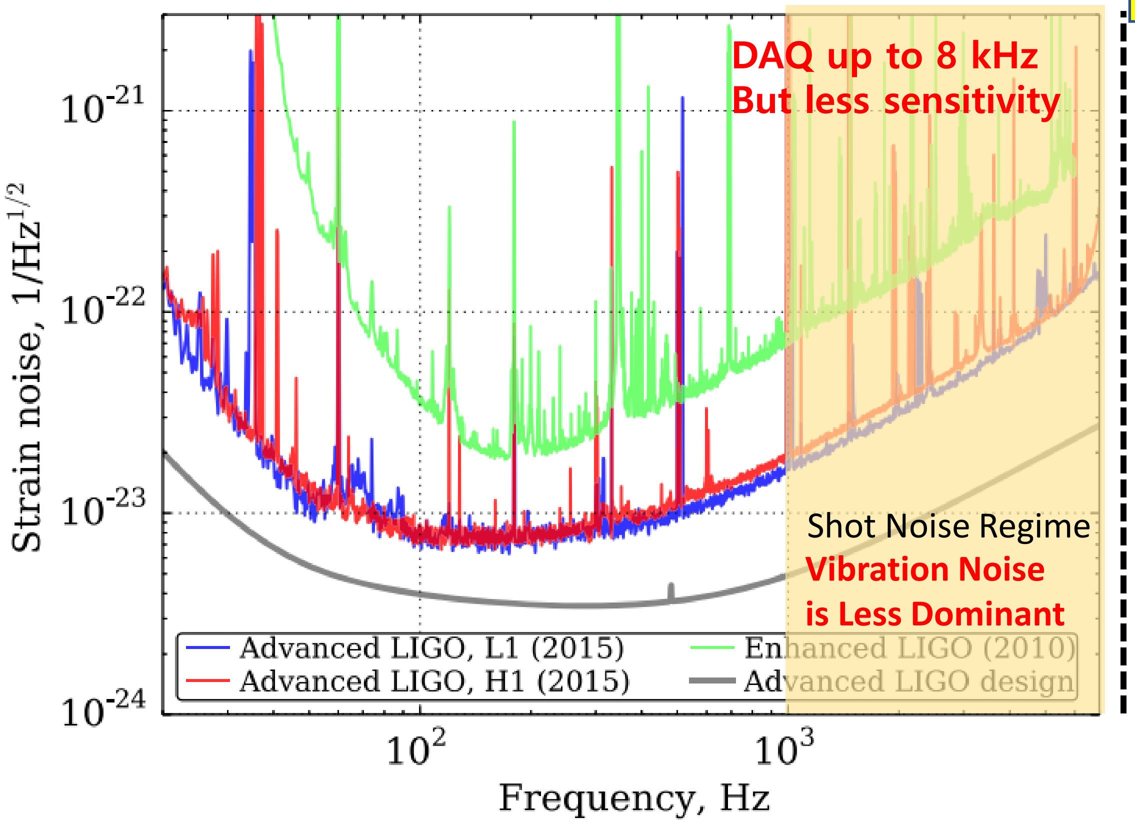

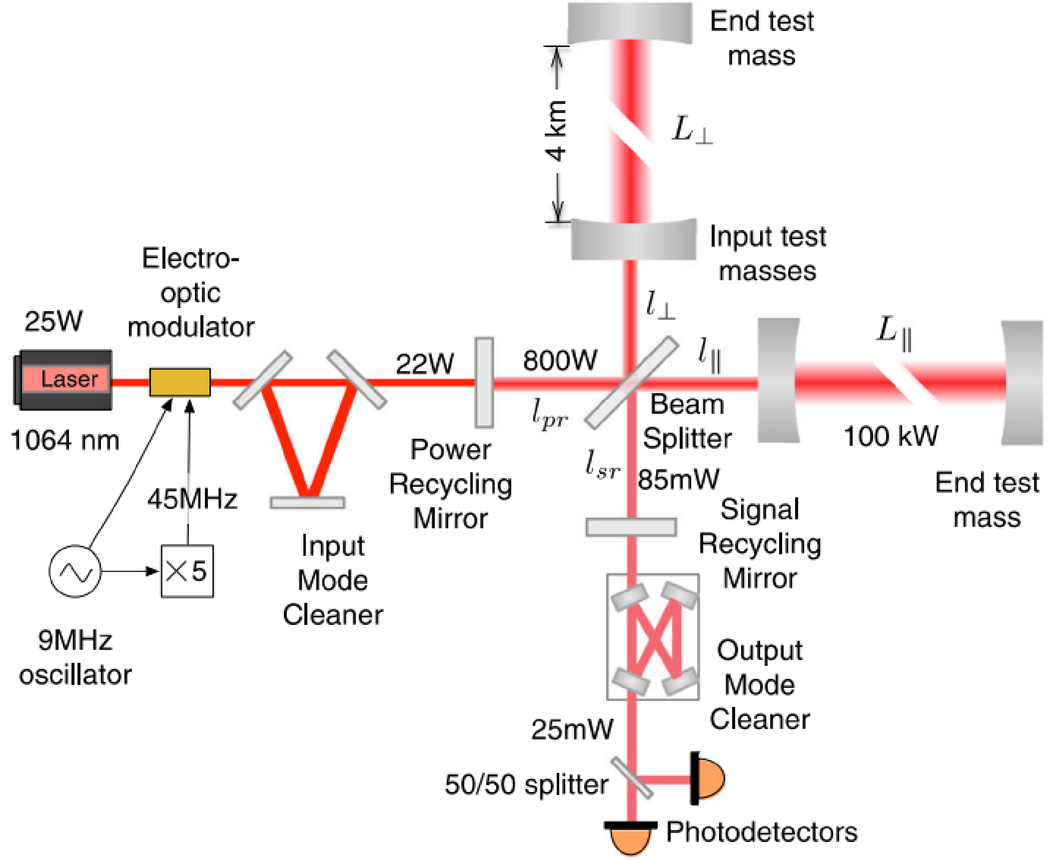

SQUID Readout

Motivation: Gravitational Wave Detection

Extend Detection Frequency O(10 kHz)

PHYSICAL REVIEW D 93, 112004 (2016)

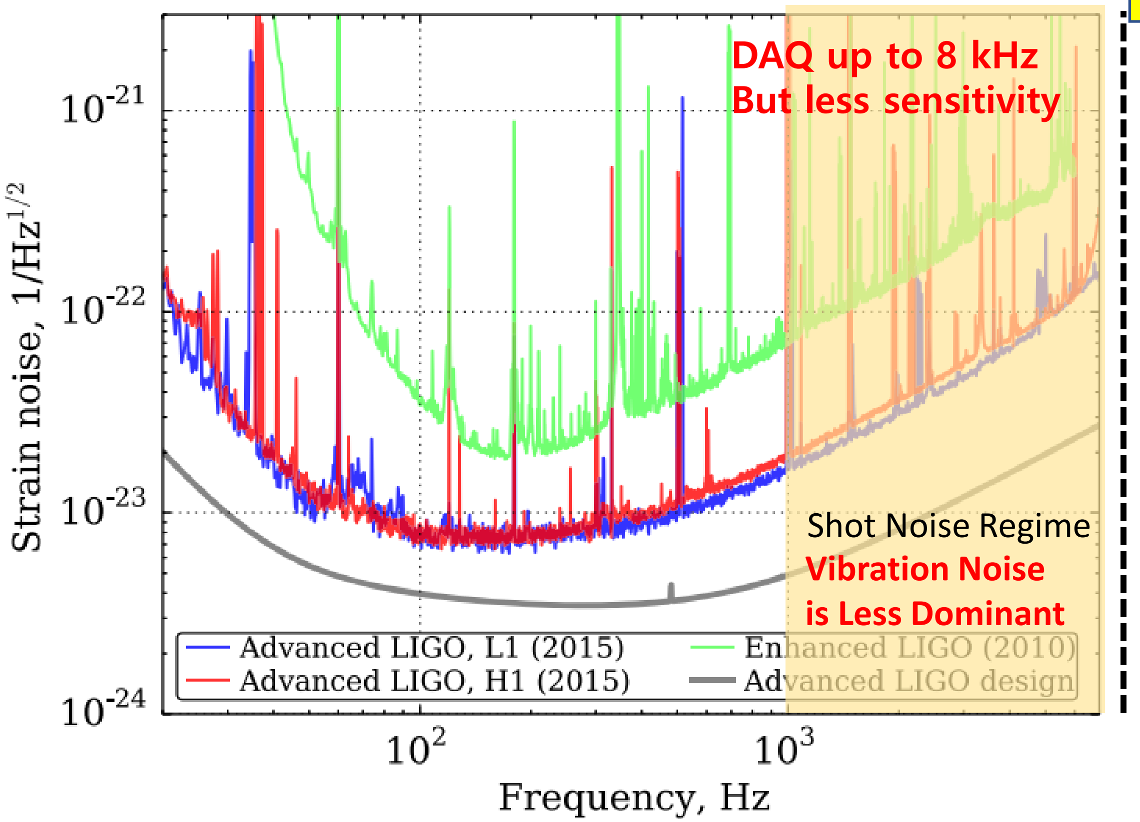

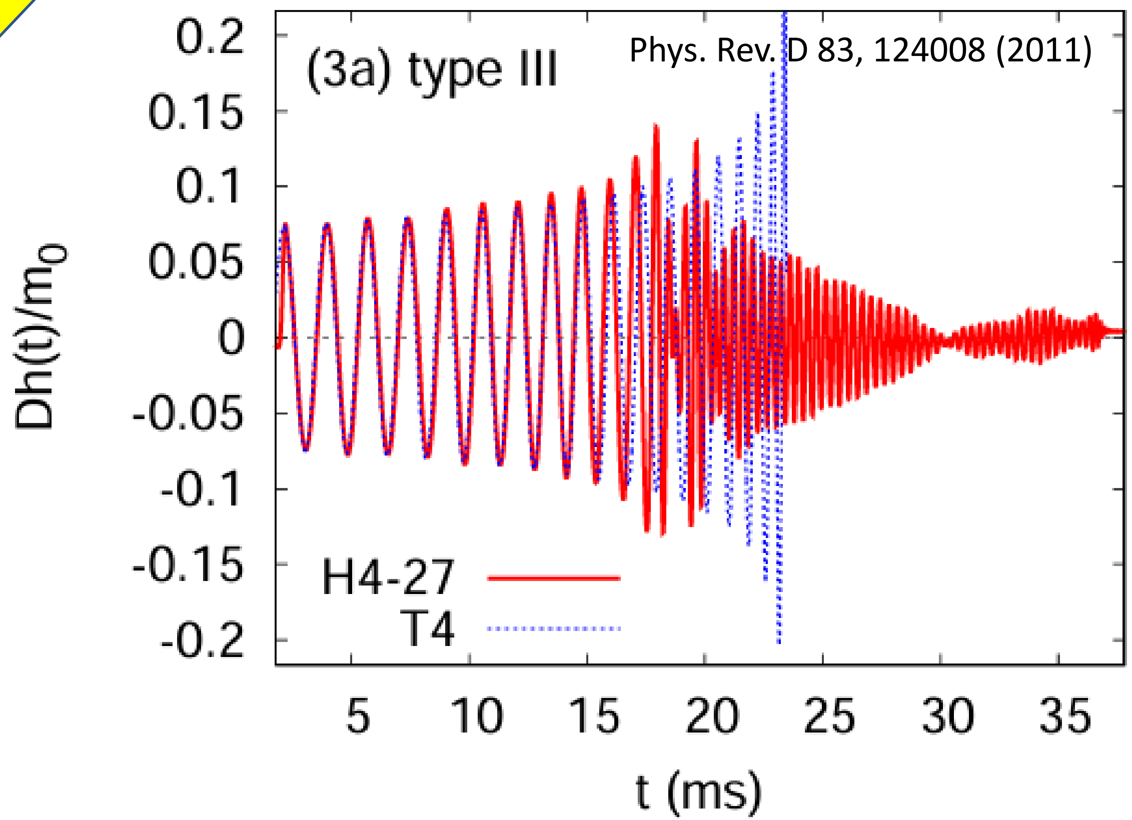

Neutron Star Binary Signal Can Give kHz Gravitational Wave Signal

SQUID Readout

Motivation: Gravitational Wave Detection

Extend Detection Frequency O(10 kHz)

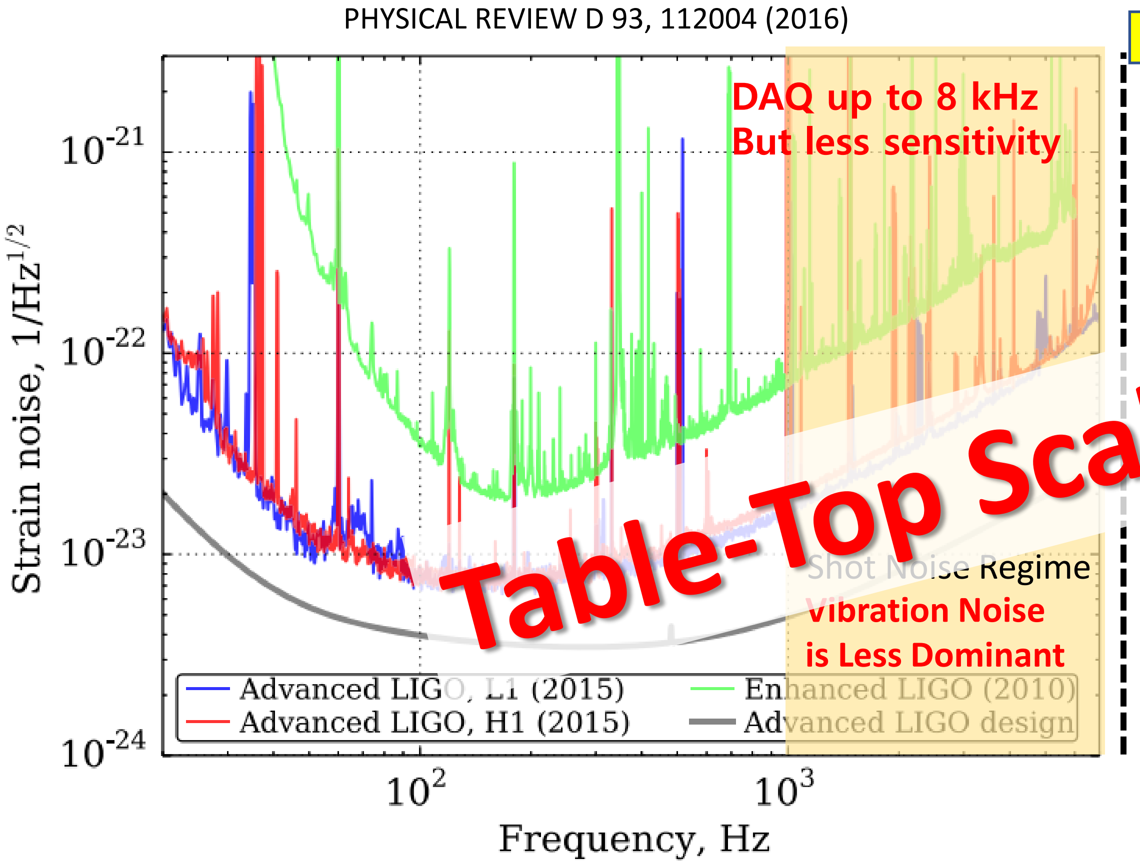

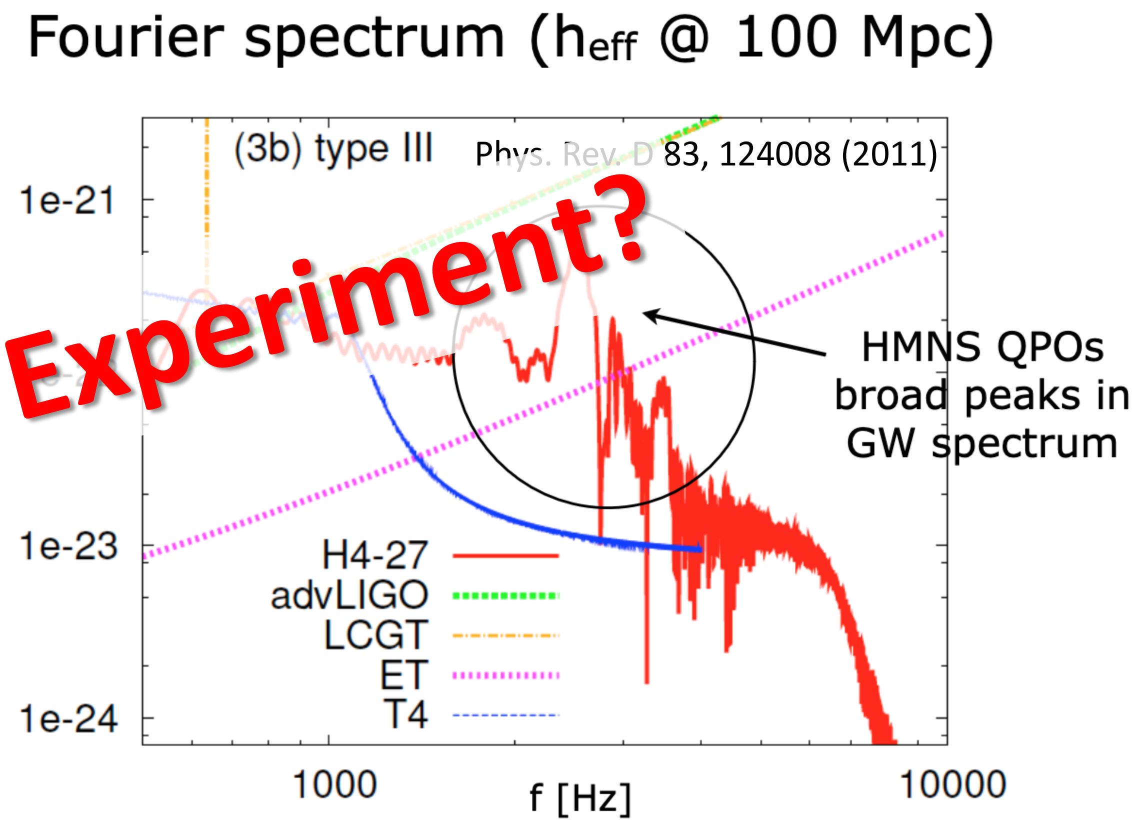

Table-Top Scale Experiment?

Higher Frequency Signals up to 10 kHz

SQUID Readout

Motivation: Bar Detector with SQUID Readout

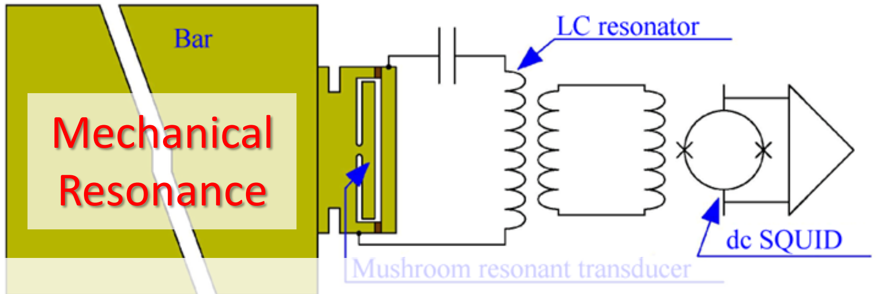

Signal ∝ Mass x Length x Q_{mech}

Phys. Rev. D 82, 022003 (2010)

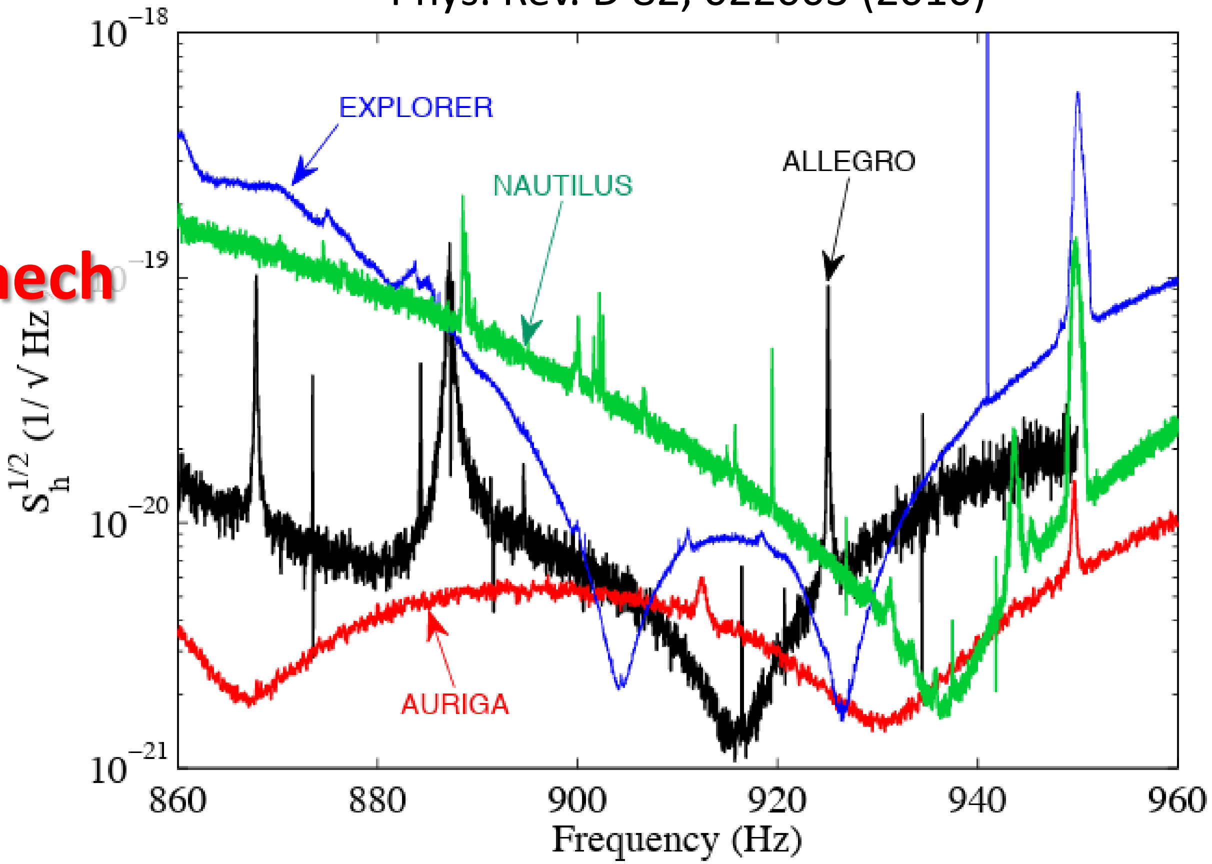

SQUID Readout

Magnetic Field Detector with SQUID Readout

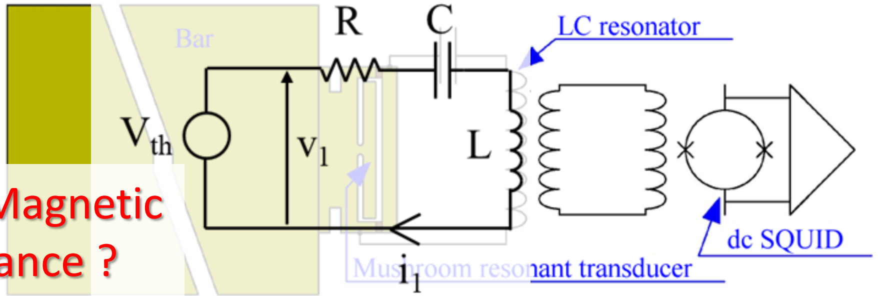

Electro-Magnetic Resonance ?

Pierluigi Fortini, Enrico Montanari, **Antonello Ortolan**, Gerhard Schäfer, Gravitational Wave Interaction with Normal and Superconducting Circuits, Annals of Physics, Volume 248, Issue 1, (1996)

Phys. Rev. D 82, 022003 (2010)

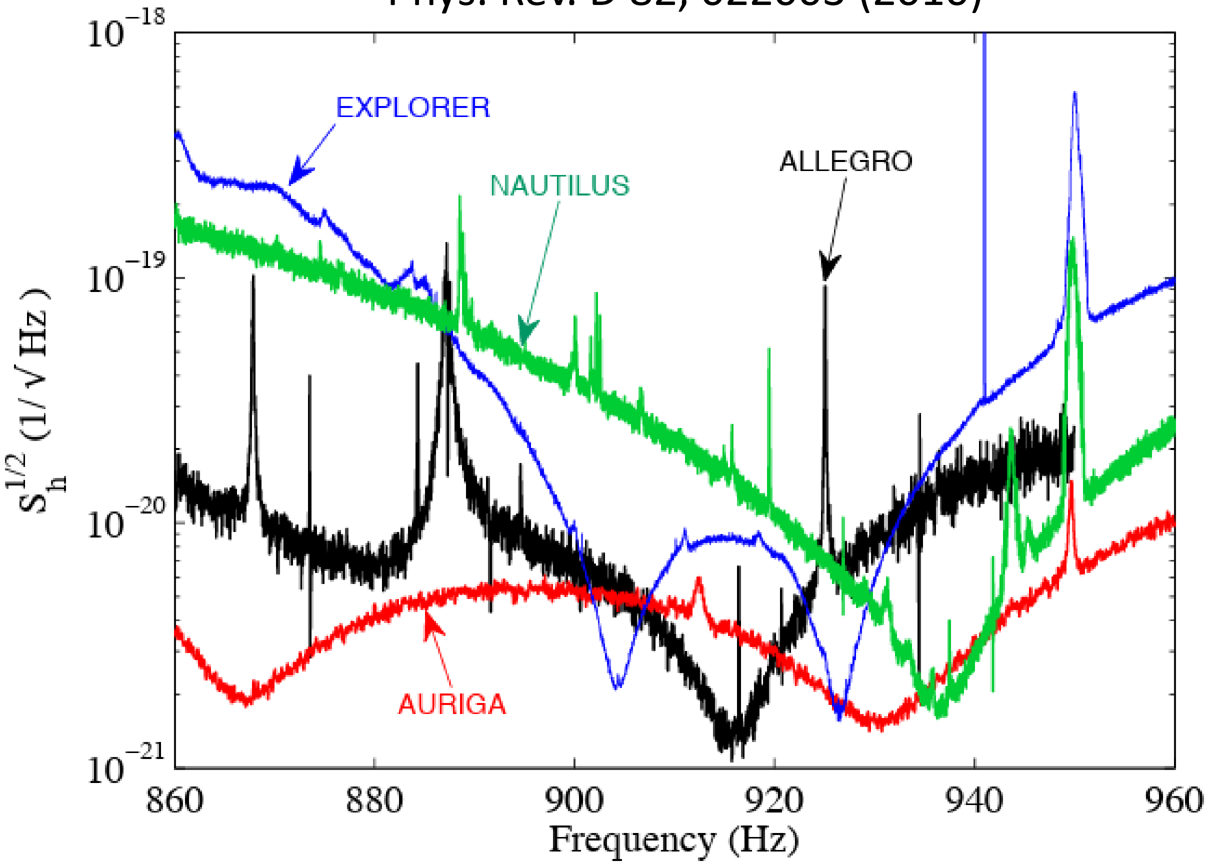

SQUID Readout

Magnetic Field Detector with SQUID Readout

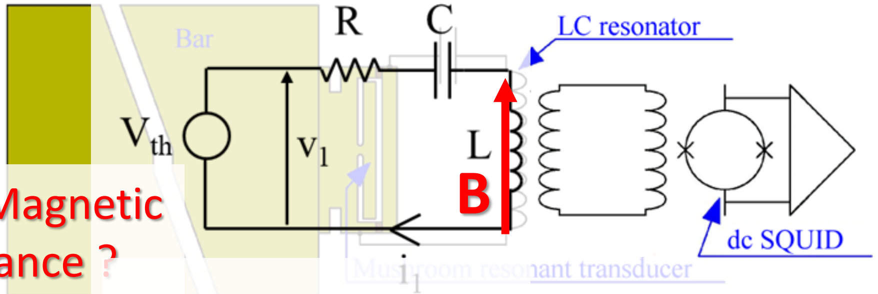

Electro-Magnetic Resonance ?

Signal ∝ B x A_{pickup}

Phys. Rev. D 82, 022003 (2010)

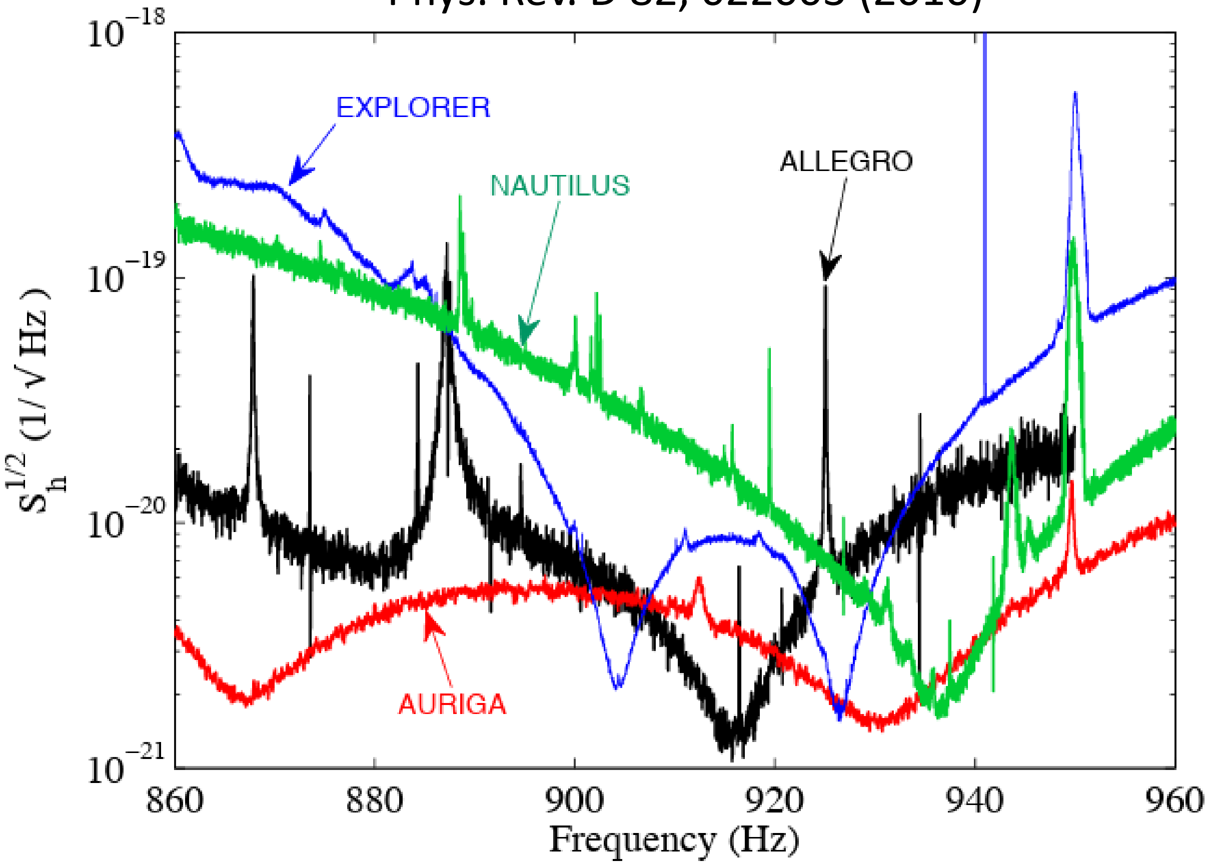

SQUID Readout

Magnetic Field Detector with SQUID Readout

$$\lambda_{GW}(\sim 10\ km) \gg \lambda_{Det}(\sim 1\ m)$$

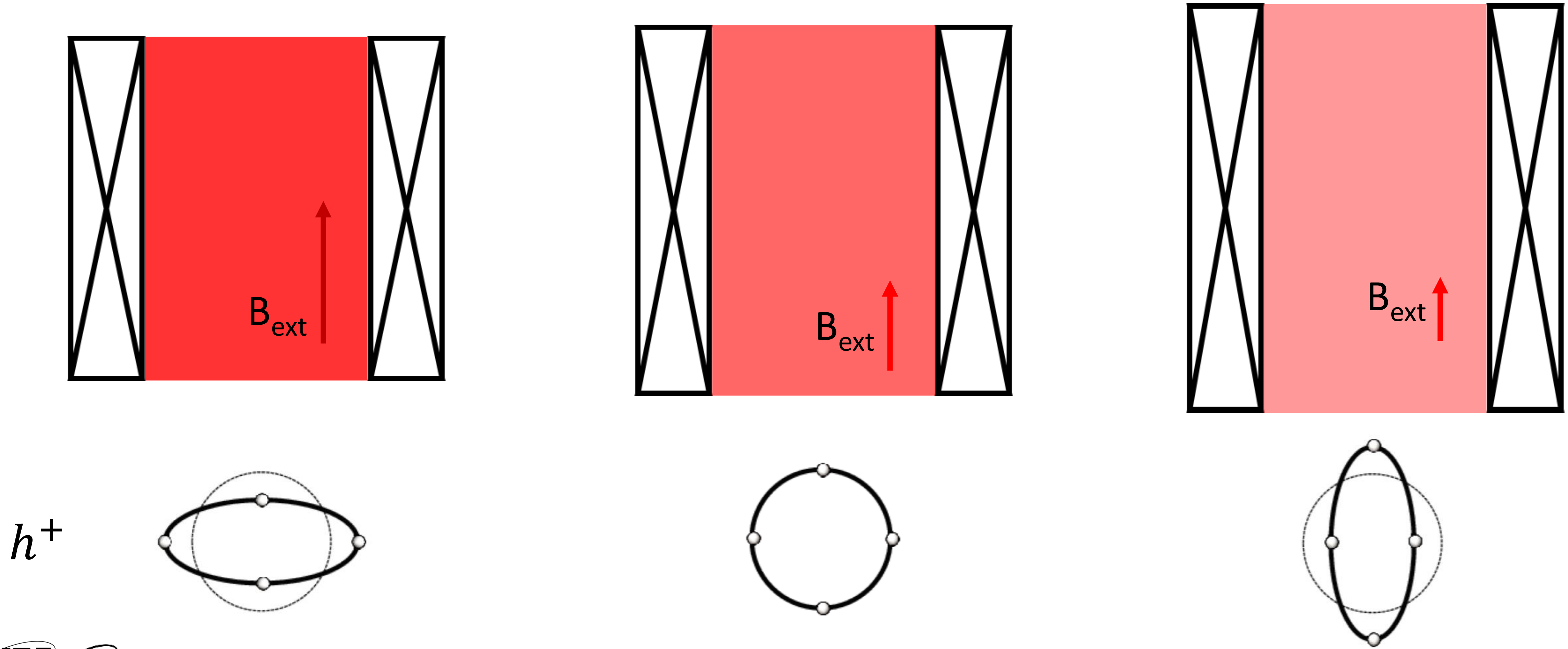

SQUID Readout

Magnetic Field Detector with SQUID Readout

$$\lambda_{GW}(\sim 10\ km) \gg \lambda_{Det}(\sim 1\ m)$$

$$\delta B_z = B_0 h_{GW} \sin^2\theta \cos 2\psi$$

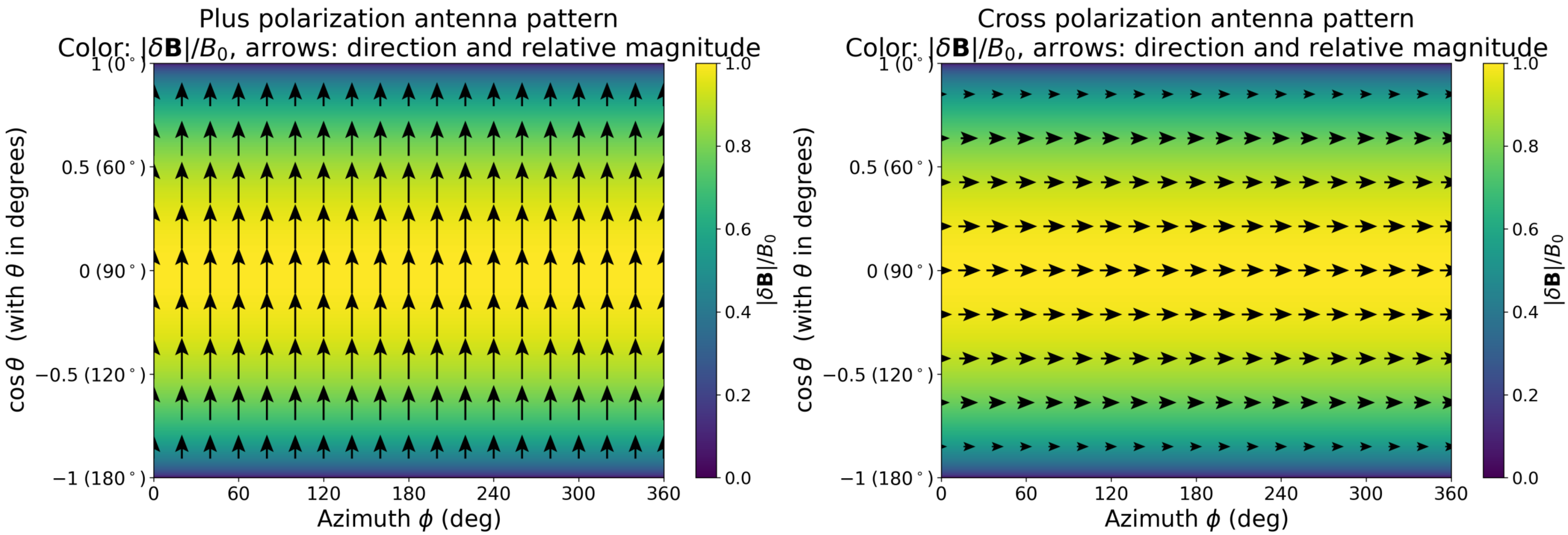

SQUID Readout

Motivation: Bar Detector with SQUID Readout

L. Baggio, M. Bignotto, M. Bonaldi, M. Cerdonio, L. Conti, **P. Falferi**, N. Liguori, A. Marin, R. Mezzena, **A. Ortolan**, S. Poggi, G. A. Prodi, F. Salemi, G. Soranzo, L. Taffarello, G. Vedovato, A. Vinante, S. Vitale, and J. P. Zendri, "3-mode detection for widening the bandwidth of resonant gravitational wave detectors," *Physical Review Letters* **94**, 241101 (2005).

Mechanical Resonant of Bar + Transducer Resonance + Electro Magnetic Mode

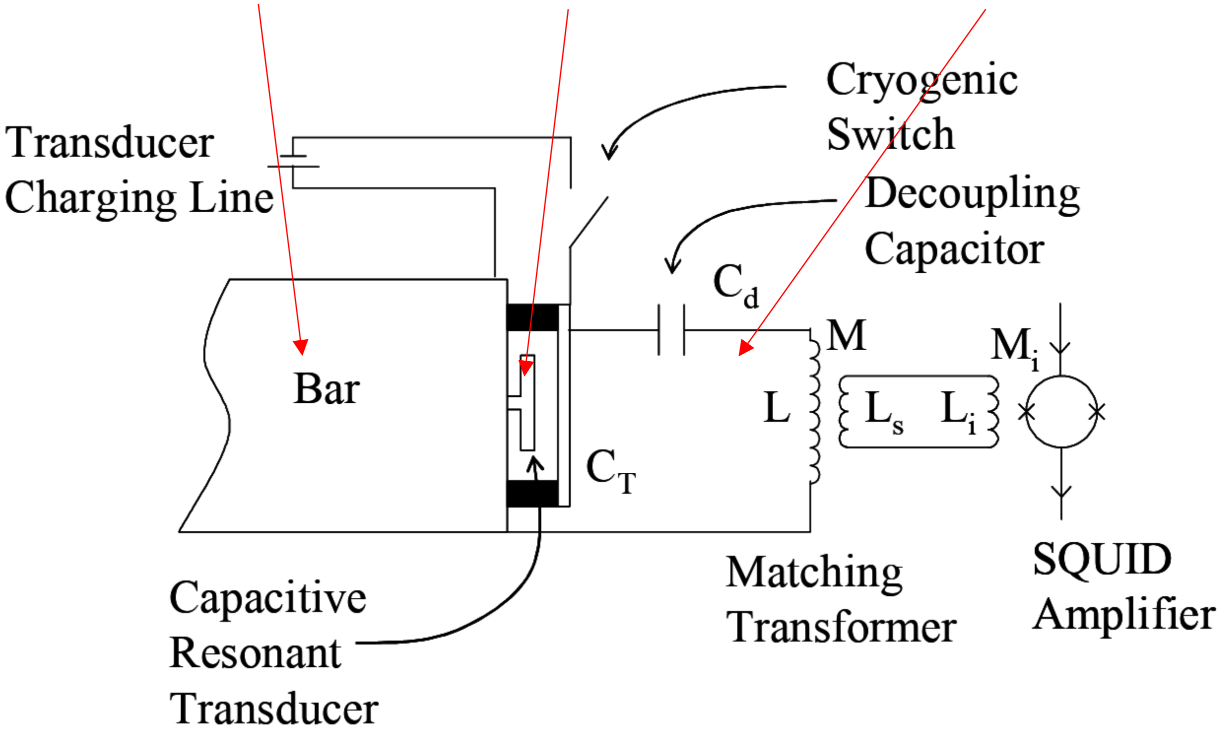

SQUID Readout

SQUID Readout for 100 Hz Bandwidth Detection

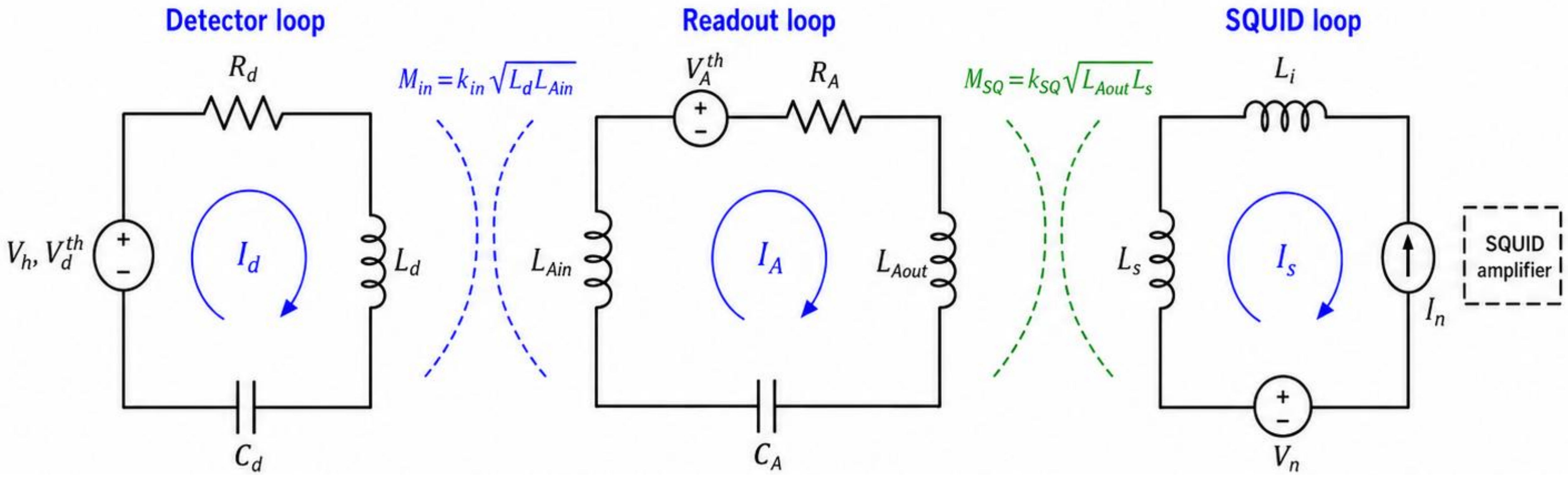

SQUID Readout

SQUID Readout for 100 Hz Bandwidth Detection

Signal source:

$$V_h = i\omega\, NABh$$

Detector impedance:

$$Z_d(\omega) = R_d + i\omega L_d + \frac{1}{i\omega C_d}$$

Readout impedance:

$$Z_A(\omega) = R_A + i\omega\left(L_{Ain} + L_{Aout}\right) + \frac{1}{i\omega C_A}$$

SQUID-loop impedance:

$$Z_s(\omega) = R_s + i\omega\left(L_s + L_i\right)$$

Measured SQUID flux:

$$\Phi_{meas} = L_i\left(I_s + I_n\right)$$

Loop-current vector:

$$I = \left(I_d,\ I_A,\ I_s\right)^T$$

Loop equations:

$$\begin{pmatrix} Z_d & i\omega M_{in} & 0 \\ i\omega M_{in} & Z_A & i\omega M_{SQ} \\ 0 & i\omega M_{SQ} & Z_s \end{pmatrix} \begin{pmatrix} I_d \\ I_A \\ I_s \end{pmatrix} = \begin{pmatrix} V_h + V_d^{th} \\ V_A^{th} \\ V_n \end{pmatrix}$$

Strain-noise model:

$$\mathcal{D}_3(\omega) = Z_s(\omega)\left[Z_d(\omega)Z_A(\omega) + \omega^2 M_{in}^2\right] + \omega^2 M_{SQ}^2 Z_d(\omega)$$

$$S_{hh} = S_d + S_A + S_{ba} + S_{imp}$$

$$S_d = \frac{4k_B T_d R_d}{\omega^2 (NAB)^2} \qquad S_A = \frac{|Z_d|^2\, 4k_B T_A R_A}{\omega^4 (NAB)^2 M_{in}^2}$$

$$S_{ba} = \frac{\left|Z_d Z_A + \omega^2 M_{in}^2\right|^2 S_{V_n}}{\omega^6 (NAB)^2 M_{in}^2 M_{SQ}^2} \qquad S_{imp} = \frac{|\mathcal{D}_3|^2 S_{I_n}}{\omega^6 (NAB)^2 M_{in}^2 M_{SQ}^2}$$

SQUID Readout

Strain Sensitivity

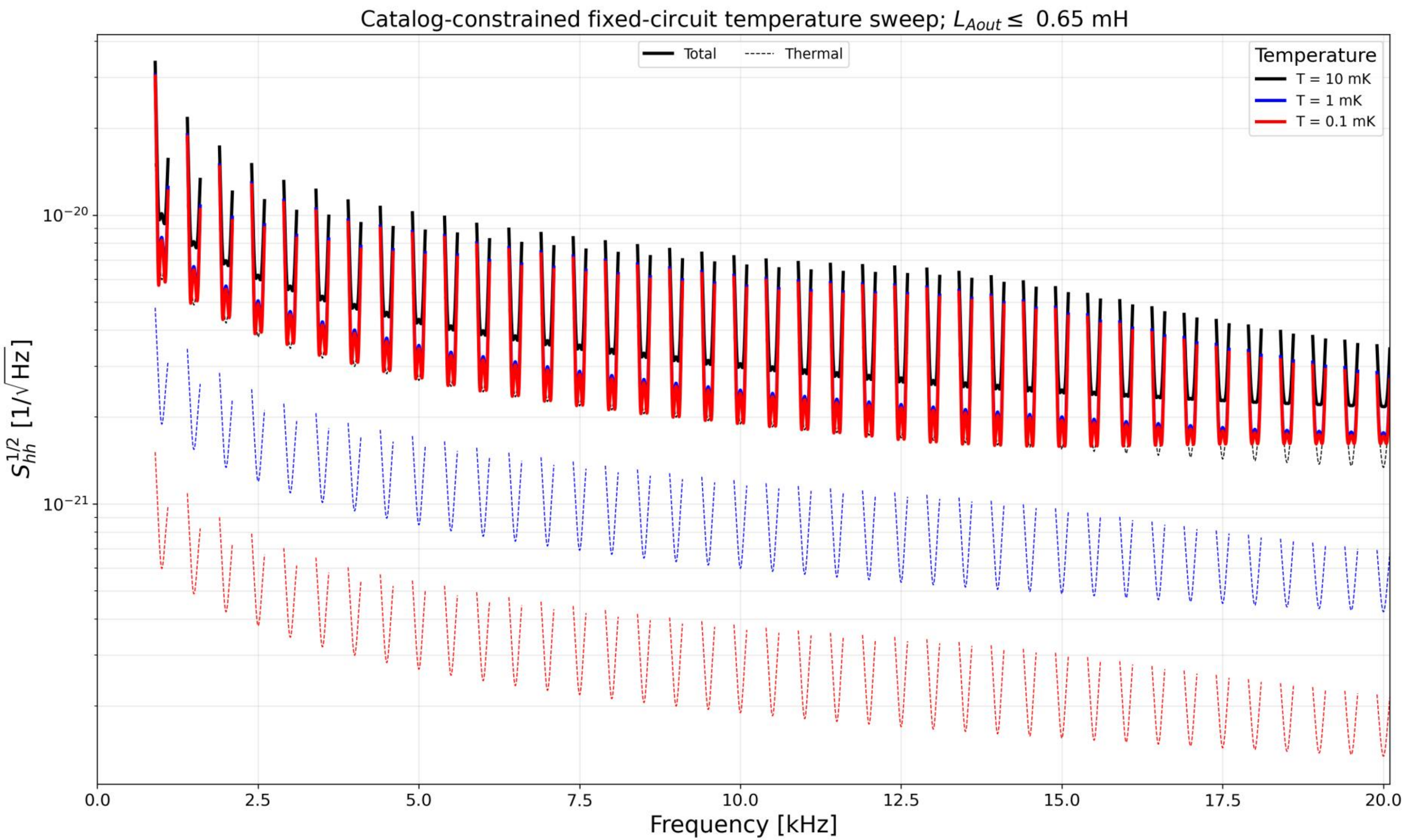

SQUID Readout

Superconducting LC Resonator

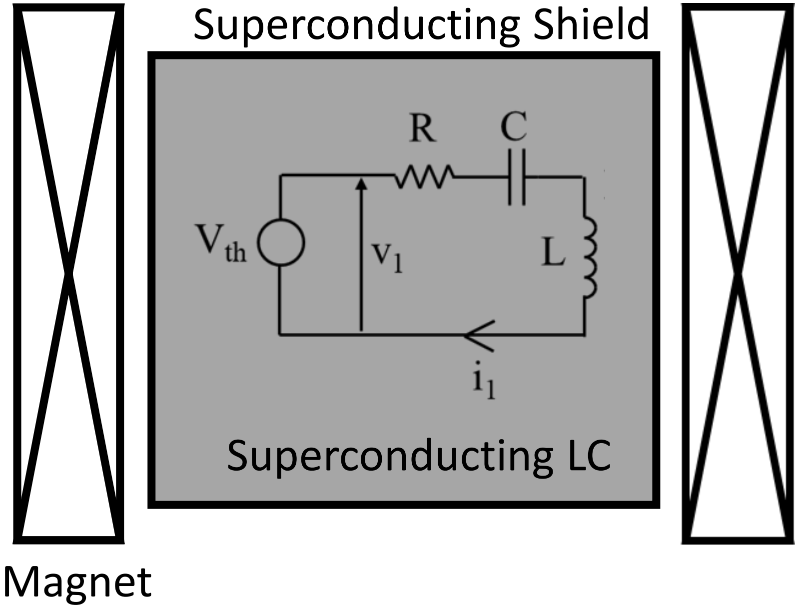

Q = 500,000 at 1.5 kHz

SQUID Readout

Piezoaxionic Effect

A. Arvanitaki, A. Madden, K. Van Tilburg, The Piezoaxionic Effect, arXiv:2112.11466

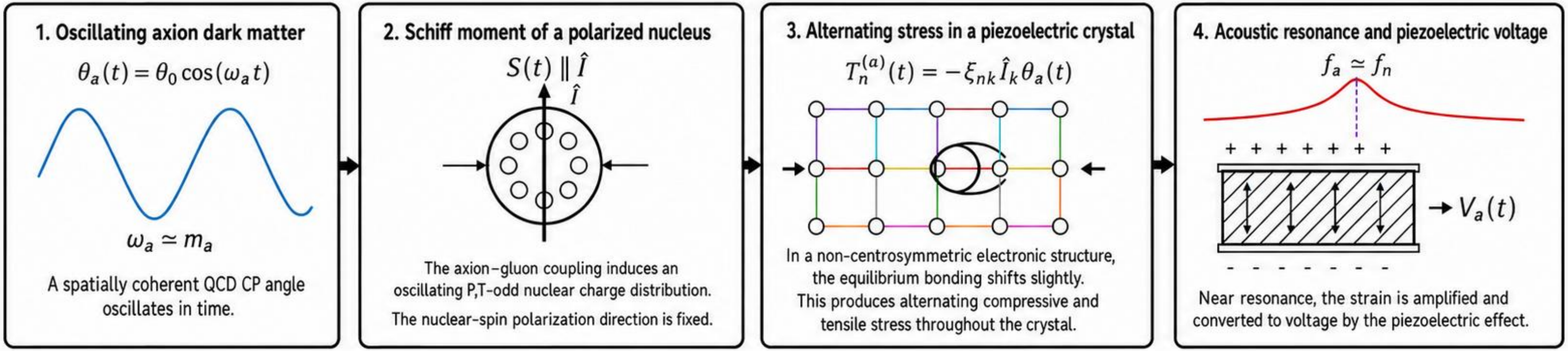

Macroscopic constitutive equations of the crystal

$$T = c^D S - h^T D - \xi \hat{I} \theta_a$$
$$E = -hS + \beta^S D - \zeta \hat{I} \theta_a$$

Piezoaxionic channel: the ξ term drives stress → acoustic resonance → the piezoelectric *h term* generates an electrical signal.

Electroaxionic auxiliary channel: *the ζ term creates a direct electric field,* but it does *not receive mechanical resonant enhancement.*

Signal frequency set by the axion mass

$$f_{\text{sig}} = \frac{\omega_a}{2\pi} \simeq \frac{m_a c^2}{h}$$
$$f_{\text{sig}} \simeq 241.8\ \text{MHz} \times \left(\frac{m_a}{\mu\text{eV}}\right)$$

The mechanical resonance is tuned to this axion-induced signal freqency.

For 10^{-11} eV $\lesssim m_a \lesssim 10^{-7}$ eV, the corresponding signal frequency is about 2.4 kHz to 24 MHz.

Summary

Status and Prospects of QUAX-PD/LNL

- QUAX-LNL is searching for axion dark matter near 10 GHz, with the 2025–2026 data analysis curre ntly in progress.
- Future upgrades include a wider-tuning, higher-Q cavity, a 14 T magnet, and an optimized TWPA to improve sensitivity and scan speed.
- The SMPD program aims to go beyond the standard quantum limit through single-microwave-photo n counting.
- SQUID-based readout activities extend QUAX searches toward kHz-frequency axion and gravitation al-wave signals.

Summary

Status and Prospects of QUAX-PD/LNL

QUAX Padova / Legnaro

F. Calaon
G. Ruoso, R. Di Vora, E. Berto, G. Carugno, A. Lombardi
C. Braggio M. Tessaro

D. Ahn, D. Maiello, A. Ortolan
G. Sardo Infirri

QUAX Frascati
D. Alesini, A. D'Elia, D. Di Gioacchino, C. Gatti, C. Ligi, G. Maccarrone, A. Rettaroli, and S. Tocci

QUAX Grenoble
G. Cappelli, M. Esposito, A. Ranadive, N. Roch

QUAX Trento
P. Falferi

QUAX Salerno
U. Gambardella, D. D'Agostino

32

Grazie per l’ascolto. ☺

Thank you for listening!